Journal of South American Earth Sciences xxx (2015) 1–15

Contents lists available at ScienceDirect

Journal of South American Earth Sciences

journal homepage: www.elsevier.com/locate/jsames

Gradients from GOCE reveal gravity changes before Pisagua Mw = 8.2 and Iquique Mw = 7.7 large megathrust earthquakes

Orlando Álvarez [a, b, *], Silvina Nacif [a, b], Silvana Spagnotto [b, c], Andres Folguera [b, d], Mario Gimenez [a, b], Mohamed Chlieh [e], Carla Braitenberg [f]

[a] Instituto Geofísico y Sismológico Ing. Volponi, Universidad Nacional de San Juan, Argentina
[b] Consejo Nacional de Investigaciones Científicas y Técnicas, Argentina
[c] Departamento de Física, Universidad Nacional de San Luis, San Luis, Argentina
[d] INDEAN – Instituto de Estudios Andinos "Don Pablo Groeber", Departamento de Cs. Geológicas, FCEN, Universidad de Buenos Aires, Argentina
[e] Géoazur, IRD UR 082, CNRS UMR 6526, Université de Nice Sophia-Antipolis, Observatoire de la Côte d'Azur, Valbonne, France
[f] Dipartimento di Matematica e Geoscienze, Universita di Trieste, Via Weiss 1, 34100 Trieste, Italy

ARTICLE INFO

Article history:
Received 28 December 2014
Received in revised form
17 September 2015
Accepted 21 September 2015
Available online xxx

Keywords:
Vertical gravity gradient
Megathrust earthquakes
Earthquake interaction
Forecasting, and prediction
Subduction
Continental margins
South Andes

ABSTRACT

Considerable improvements in the measurement of the Earth gravity field from GOCE satellite mission have provided global gravity field models with homogeneous coverage, high precision and good spatial resolution. In particular, the vertical gravity gradient (***Tzz***), in comparison to the classic Bouguer anomaly, defines more accurately superficial mass heterogeneities. Moreover, the correction of these satellite-derived data from the effect of Earth topographic masses by means of new techniques taking into account the Earth curvature, improves results in regional analyses. In a recent work we found a correlation between Tzz and slip distribution for the 2010 Maule Mw = 8.8 earthquake. In the present work, we derive the vertical gravity gradient from the last GOCE only model, corrected by the topographic effect and also by the sediments on depocenters of the offshore region at the Peru–Chile margin, in order to study a spatial relationship between different lobes of the gravity derived signal and the seismic sources of large megathrust earthquakes. In particular, we analyze this relation for the slip models of the 1996 Mw = 7.7 Nazca, 2001 Mw = 8.4 Arequipa, 2007 Mw = 8.0 Pisco events and for the slip models of the 2014 Mw = 8.2 Pisagua and Mw = 7.7 Iquique earthquakes from Schurr et al. (2014), including the previously analyzed 2010 Mw = 8.8 Maule event. Then we find a good correlation between vertical gravity gradients and main rupture zones, correlation that becomes even stronger as the event magnitude increases. Besides this, a gravity fall in the gravity gradient was noticed over the area of the main slip patches at least for the two years before 2014 Mw = 8.2 Pisagua and Mw = 7.7 Iquique earthquakes. Additionally, we found temporal variations of the gravity field after 2010 Mw = 8.8 Maule event, related to the main patches of the slip distribution, and coseismic deformation. Therefore, we analyzed vertical gravity gradient field variations as an indirect measure of the variable seismic coupling finding a potential relationship between Tzz and the seismic b-value. These relationships exemplify the strong potential of the satellite only derived models as a predictive tool to determine potential seismic energy released in a subduction segment, determining the potential size of a potential rupture zone, and in particular internal slip distribution that allows inferring coseismic displacement field at surface.

1. Introduction

Prediction of potential seismic energy after major earthquakes and distribution of coseismic displacements in active tectonic settings have been major tasks in the last years from remote sensing and field surveys, including measurements of gravity field and ground deformations (e.g. Dreger and Kaverina, 2000; Peltzer et al., 2001; among others). The Peru–Chile subduction zone, where

* Corresponding author. Mariano Moreno 240 (S) dpto:6 Rivadavia, San Juan, Argentina.
E-mail addresses: orlando_a_p@yahoo.com.ar, orlando.alvarez@conicet.gov.ar (O. Álvarez), nacif.silvina@gmail.com (S. Nacif), pampa113@gmail.com (S. Spagnotto), andresfolguera2@yahoo.com.ar (A. Folguera), gimmario@gmail.com (M. Gimenez), chlieh@geoazur.unice.fr (M. Chlieh), berg@units.it (C. Braitenberg).

http://dx.doi.org/10.1016/j.jsames.2015.09.014
0895-9811/

about one third of the total last century worldwide seismic energy was released, is characterized by the occurrence of large megathrust earthquakes at the contact between the Nazca and South American plates. Gravity measurements have proven to be very useful for studying the structure, plate geometry and seismic segmentation of the interplate megathrust (Llenos and Mc Guire, 2007; Sobiesiak et al., 2007; Tassara, 2010; Álvarez et al., 2014, 2015a,b; Maksymowicz et al., 2015).

In particular, satellite gravity data have been used in offshore and onshore studies monitoring density variations through the forearc above a subduction zone. Song and Simons (2003) were the first who correlated strong negative gravity anomalies parallel to the trench with maximum slips of large earthquakes. Then Wells et al. (2003) established a link between forearc gravity lows, basins developed on the frontal accretionary prism, enhanced subduction erosion and large coseismic slips. From these analyses, negative gravity anomalies seem to be related to areas of high-shear traction on the interplate interface, in association with an increment in the effective friction coefficient (Llenos and Mc Guire, 2007). More locally, Sobiesiak et al. (2007) observed positive correlations between seismic *b-value*, isostatic residual gravity anomalies and geologic structures along the Northern Chilean margin. Similarly, Tassara (2010) correlated gravity and seismogenic structure of the Chilean margin, influenced by the varying vertical stress loading the subduction zone due to a heterogeneous density structure of the upper plate forearc. Following this hypothesis, Álvarez et al. (2014) have found a general agreement between lows of vertical gravity gradients derived from GOCE-satellite data (Gravity Field and Steady State Ocean Circulation Explorer) and the location of higher slips on seismic sources of the 1960 Mw = 9.6 Valdivia and 2010 Mw = 8.8 Maule earthquakes that occurred in south-central Chile. A more recent work of Maksymowicz et al. (2015) based on 2-D gravity modeling showed that the highest slip during the Maule earthquake is located in a segment of the margin characterized by low densities in the continental wedge, low vertical loading over the seismogenic contact, a well-developed shelf basin, and low taper angles consistent with a low effective basal friction coefficient.

In this work, seismic sources of recent Mw > 7.5 earthquakes that occurred next to the Arica bend region (14°S to 24°S) in the Central Andes (Fig. 1) are first compared to the topography and sediment corrected vertical gravity gradient obtained from the GOCE model ***GO_CONS_GCF_2_TIM_R5*** (Pail et al., 2011; Brockmann et al., 2014). Then, vertical gravity gradient measurements are locally compared with the seismic sources of other large Peruvian events occurred in 1996 (Nazca, Mw = 7.7), 2001 (Arequipa, Mw = 8.4) and 2007 (Pisco, Mw = 8.0). The slip distribution models of the April 1st 2014 Mw = 8.2 Pisagua earthquake and its main aftershock on April 3rd 2014 Mw = 7.8 Iquique that ruptured partially the northern Chile seismic gap (Schurr et al., 2014) are also compared with vertical gravity gradient measurements. The GOCE only model *GO_CONS_GCF_2_TIM_R4* and the following *TIM_R5* were obtained by the Time-wise method and cover different time data span, constituting a good tool for studying Earth gravity field changes. The data span for both models allows to detect gravity field changes after 2010 Mw = 8.8 Maule and before the 2014 Mw = 8.2 Pisagua and 2014 Mw = 7.7 Iquique earthquakes. In this work we analyzed the probable relationships/correlations between slight Earth gravity field changes, detected by means of GOCE gravity gradients, and different parameters as the degree of seismic coupling and seismic b-value.

2. Seismotectonic setting

The interplate zone along the Peru-Chilean trench has been affected by large megathrust earthquakes, being some of them the largest recorded in the world, including the 2010 Mw = 8.8 Maule earthquake in central Chile, and the 1960 Mw = 9.5 Valdivia earthquake in southern Chile. These earthquakes are produced within the area of contact between the Nazca and South American plates. The Nazca Plate subducts obliquely beneath the western margin of Central and Southern South America (Fig. 1), defining the Peru–Chile trench, located at about 150 km off the coast of Peru and Chile (Lindquist et al., 2004; Völker et al., 2006). Near the Arica bend, the subducting oceanic Nazca Plate is associated with a series of bathymetric highs: the Nazca ridge that intersects the trench at a latitude of 15°S, the Nazca Fracture zone at 17°S, and the Iquique ridge at about ~21°S (Fig. 1). The northern Chilean margin is characterized as an erosive margin with a trench that is virtually starved of sediments, exhibiting a very steep offshore forearc (von Huene and Scholl, 1991; Adam and Reuther, 2000; Lamb and Davis, 2003; Völker et al., 2006; Tassara et al., 2006). Bangs and Cande (1997) measured approximately ~0.5 km of sediment filling at the trench north of 21°S, while to the south less than 0.1 km are present up to 27°S. The lack of sediments in the trench at these northern latitudes is explained by little precipitation during the past 20 Ma on the western Andean slope (Scholl et al., 1970; Hartley and Jolley, 1995), with a minimal supply in the last 10 Ma as a consequence of

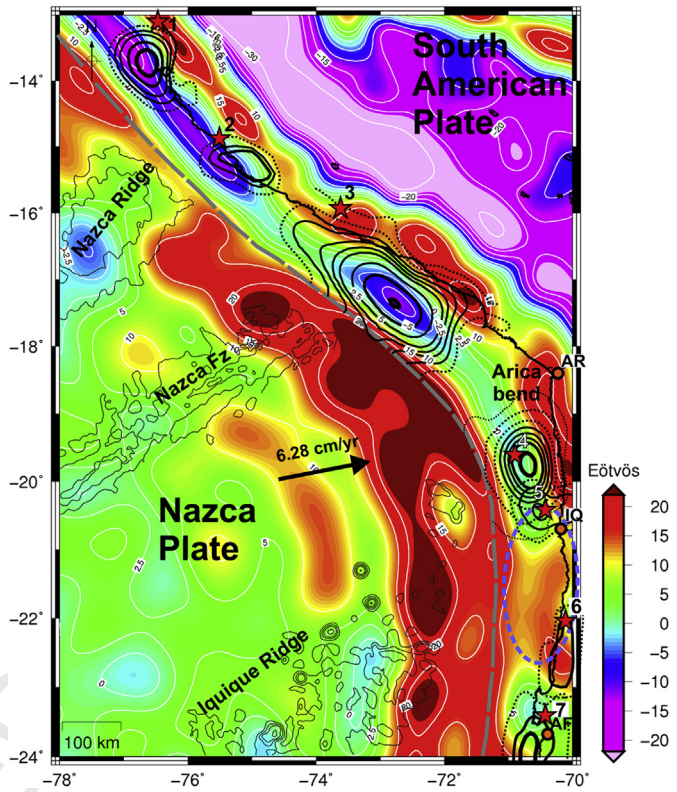

Fig. 1. Topography corrected vertical gravity gradient in the Central Andes and adjacent Nazca plate, obtained from GOCE satellite-only model **GO_CONS_GCF_2_TIM_R5** from Brockmann et al. (2014) (**Tzz** is indicated with white contours). Convergence between Nazca-South American plates (black arrow) is from Kendrick et al. (2003) (the Perú-Chilean trench is indicated with a gray dashed line and the bathymetric highs mentioned in the text with thin black lines). Superimposed slip distributions for the 2007 Mw = 8.0 **Pisco** (**1**); 1996 Mw = 7.7 **Nazca** (**2**), 2001 Mw = 8.4 **Arequipa** (**3**), 2007 Mw = 7.7 **Tocopilla** (**6**) and 1995 Mw = 8.1 **Antofagasta** (7) from Chlieh et al. (2004, 2011) and for the 1st April 2014 Mw = 8.2 **Pisagua** (**4**) and 3rd April 2014 Mw = 7.7 **Iquique** (**5**) from Schurr et al. (2014). References: Red stars are the epicenters for the different earthquakes shown in this figure. **AR**: Arica, **IQ**: Iquique, **AF**: Antofagasta. Blue dashed line: 1877 Mw = 8.6 reduced zone from Metois et al. (2013). (For interpretation of the references to colour in this figure legend, the reader is referred to the web version of this article.)

extreme arid conditions after the uplift of the Altiplano (Garzione et al., 2008). Subduction erosion processes in this region, related to the morphological roughness of the oceanic plate and the lack of sediments within the trench, have been proposed as the major control in arc eastward migration in the last 100 My (Stern, 1991; Haschke et al., 2006; Kay et al., 2005).

In Southern Peru, large megathrust earthquakes with moment magnitude of $8.4 \geq Mw \geq 8.8$ occurred in 1604, 1687, 1784 and 1868 (Dorbath et al., 1990; Kelleher, 1972; Nishenko, 1985). However, only indirect estimations of their approximate rupture length and moment magnitude are available. Contrastingly, since the advent of modern space-based geodesy and broadband seismology, the seismic sources of recent large megathrust earthquakes, as the 1996 $Mw = 7.7$ Nazca, 2001 $Mw = 8.4$ Arequipa, and 2007 $Mw = 8.0$ Pisco earthquakes, have been studied in detail (Pritchard et al., 2007; Sladen et al., 2010; Chlieh et al., 2011) (Fig. 1). To the south, along the northern Chile margin, the largest historical earthquake occurred in 1877 (Iquique event) with magnitude Mw ~ 8.5–8.8 (Lomnitz, 2004), and estimated rupture zone from Arica to Antofagasta. This zone was recognized as the Iquique seismic gap in northern Chile, with a return period varying from ~111 to 264 yr (Nishenko, 1985; Comte and Pardo, 1991; Chlieh et al., 2011). The southern part of this gap was recently affected by the 2007 $Mw = 7.8$ Tocopilla earthquake. Metois et al. (2013) using geodetic measurements reduced the previously proposed rupture zone of the 1877 earthquake (Kausel, 1986), which allowed to invert the interseismic coupling distribution on the slab interface with better precision and resolution (Fig. 1).

3. Data and method: direct modeling from satellite-derived models

The GOCE model ***GO_CONS_GCF_2_TIM_R5*** (Pail et al., 2011; Brockmann et al., 2014) is a satellite-only model combining SST-hl (high-low Satellite-to-Satellite Tracking) and ***SGG*** (Satellite Gravity Gradiometer) data. It is a GOCE-only solution in a rigorous sense since no external gravity field information is used, neither as a reference model nor for constraining the solution. This model was obtained by the Time-wise method, and is the one of the maximum degree/order ($N = 280$) from satellite-only data at this time, with an effective data volume of approx. 42 months (data period: 01/11/2009–21/10/2013). This allows obtaining a resolution of approximately $\lambda/2 \approx 2\pi R/N_{max} \approx 71$ km with R being the mean Earth radius and N_{max} the maximum degree and order of the harmonic expansion (Li, 2001; Hofmann-Wellenhof and Moritz, 2006; Barthelmes, 2009). The observed potential is obtained from the global gravity field model, from which the disturbing potential (T) is calculated after subtracting the potential field of the reference ellipsoid (WGS84) (Janak and Sprlak, 2006). The gravity gradient tensor (Marussi tensor) is obtained as the second derivatives of the disturbing potential T (e.g. Hofmann-Wellenhof and Moritz, 2006) and is composed of five independent elements. The Marussi tensor components $M = T_{ij}$ can be expressed and solved numerically in a spherical coordinate system (Tscherning, 1976; Rummel et al., 2011).

In the present work we calculate the vertical gravity gradient (***Tzz***) in terms of the spherical harmonic coefficients up to degree/order $N = 280$ for the mentioned earth gravity field model, on a regular grid of 0.05° grid cell size. The ***Tzz*** is obtained in Eötvös (10^{-4} mGal/m), as the second derivative of the disturbing potential in the radial direction. The ***Tzz*** represents a better theoretical resolution than the gravity vector for some geophysical features (Li, 2001) and allows delineating the location of an anomalous mass with better detail and accuracy than the gravity anomaly itself (Braitenberg et al., 2011). The ***Tzz*** is particularly sensitive to superficial density variations relative to gravity, although is totally insensitive to flat extended mass inhomogeneities, whereas a flat mass sums to the superficial effect of the gravity. In particular, Álvarez et al. (2014) have shown a correlation between low ***Tzz*** values and high slip areas of the 2010 Maule seismic source.

With the aim of reducing the ***Tzz*** for the gravity effect of topography, we used spherical prisms of constant density (Heck and Seitz, 2007; Wild-Pfeiffer, 2008; Grombein et al., 2013; among others), to discretize the digital terrain model and contemplate the Earth's curvature (Uieda et al., 2010). This calculation with spherical prisms is used since a planar approximation induces a considerable error (Braitenberg et al., 2011; Alvarez et al., 2012, 2013; Bouman et al., 2013; Grombein et al., 2013). The Marussi tensor components $\underline{M} = (M_{ij})$ due to the topographic masses in a spherical coordinate system are given by Tscherning (1976) and by Rummel et al. (2011). A standard density of 2.67 g cm^{-3} was used for masses above sea level and a density of 1.03 g cm^{-3} for the sea water. The potential generated by the topography is calculated from the Digital Elevation Model (ETOPO1, Amante and Eakins, 2009), using the software Tesseroids (Uieda et al., 2010; Alvarez et al., 2013), where the calculation height is 7000 m to ensure that all values are above the topography. The topographic correction amounts up to tens of Eötvös for the vertical gravity gradient, becoming higher over the highest topographic elevations and over the lowest topographic depressions such as the Peru–Chile trench.

The same method was used to perform the sediment correction, taking into account a mean density of 2.4 g cm^{-3}. These values of sediment densities were used in the region by Ranero et al. (2006) and were obtained from modeling wide angle seismic and gravity data (Sallares and Ranero, 2005). Sediment thicknesses were obtained from NGDC's global ocean sediment thickness grid from Whittaker et al. (2013), an updated version of the NGDC's original ocean sediment thickness grid from Divins (2003).

4. Results

The vertical gravity gradient (***Tzz***) allows delimiting a series of features in both the Nazca and western South American plates, as well as to study the heterogeneous density structure of the forearc region related to rupture zones associated with large earthquakes. In particular, the Nazca ridge is detected over the ocean floor by a more negative ***Tzz*** signal than the surrounding Nazca Plate, ranging from −10 to +5 Eötvös, becoming more positive near the trench (Fig. 1). The Nazca fracture zone is also identified by the ***Tzz***, presenting subdued negative values than the surrounding ocean floor, extending in the NE direction from the Nazca ridge to the trench. Similarly, to the south, the Iquique ridge is detected by a more negative ***Tzz*** signal ranging from less than −2.5 to more than +10 Eötvös. Parallel to the trench, the flexural bulge (outer rise) is denoted by a high ***Tzz*** value reaching maximum values at the Arica bend region. High positive ***Tzz*** values over the outer rise are segmented by lower ***Tzz*** values of the Nazca and Iquique ridges and the Nazca fracture zone (Alvarez et al., 2015b). This imprint on the flexural bulge related to the high oceanic features (HOF's) has also been noted at the southern Chilean margin for the Juan Fernandez ridge (Álvarez et al., 2014, 2015a) and for different Fz's related to the Chile Rise.

More locally, between the trench and the coastline, the segmented ***Tzz*** signal allows individualizing a series of negative anomalies reaching less than −20 Eötvös (Fig. 1). ***Tzz*** highlights mass inhomogeneities that could reflect along-strike variations in temperature, fluid pressure, and stresses on the subduction zone probably caused by variations in overlying forearc thickness and density. In this case the segmented ***Tzz*** signal is interpreted as the expression of low-density materials in sedimentary depocenters

Please cite this article in press as: Álvarez, O., et al., Gradients from GOCE reveal gravity changes before Pisagua Mw = 8.2 and Iquique Mw = 7.7 large megathrust earthquakes, Journal of South American Earth Sciences (2015), http://dx.doi.org/10.1016/j.jsames.2015.09.014

superimposed to the accretionary prism, as observed by Álvarez et al. (2014) for the South Central Chile region. Coseismic slips tend to concentrate beneath these gravimetric lows, being an indirect indicator of the seismogenic structure (Wells et al., 2003; Song and Simons, 2003; Tassara, 2010; Álvarez et al., 2014; Maksymowicz et al., 2015).

In this work, we compared the topography and sediment corrected vertical gravity gradient (***Tzz***) computed from GOCE (TIM_R5) model at 7000 m over the topographic masses with the seismic sources of the 2007 Mw = 8.0 Pisco (Fig. 2), 1996 Mw = 7.7 Nazca (Fig. 3), and 2001 Mw = 8.4 Arequipa (Fig. 4). Then we compared our results with the slip models for the April 1st (Fig. 5) and 3rd (Fig. 6) 2014 events from Schurr et al. (2014). In a general analysis, we found a good spatial correlation between areas of low and more negative ***Tzz*** and high seismic slip, especially for the Mw ≥ 8.0 events. North of 20°S the ***Tzz*** signal diminishes, determining a negative lobe up to 19°S (reaching less than −2.5 Eötvös). Maximum slip for the April 1st 2014 Mw = 8.2 is located between these latitudes (Schurr et al., 2014; Hayes et al., 2014). The relation between more negative Tzz and higher slip was tested in Figures 2–7. Then, we plotted the absolute value of the correlation coefficient between ***Tzz*** and slip versus the maximum slip for all the events (Fig. 8), including the 2010 Mw = 8.8 Maule event (Fig. 7), finding that when magnitude increases, the correlation between low ***Tzz*** (10^{-4} mGal/m) and high slip (m) also increases. This is particularly notorious for Mw ≥ 8.0 events, probably due to the high spatial resolution of GOCE only models (Fig. 8).

In particular, this correlation between high slips and low vertical gravity gradients for the 2010 Mw = 8.8 Maule earthquake is recently explored by Maksymowicz et al. (2015). The authors explain this relation by low densities in the continental accretionary wedge, low vertical loading over the inter-plate contact, a well-developed shelf basin and low taper angles consistent with a low effective basal friction coefficient. Then, a qualitative relation arises between high slips and low gravity signal (Wells et al., 2003; Song and Simons, 2003) and even with lower ***Tzz*** values (Álvarez et al., 2014) for most of the subduction-related events at the Peru–Chile margin (this work). Even though the main slip for the 2014 Mw = 8.2 Pisagua earthquake is correlated with a low ***Tzz*** only in the northern part, the correlation between high slips and relatively lower ***Tzz*** is still observed (Fig. 5c).

Contrastingly, the 2014 Mw = 7.7 Iquique and the 1995 Mw = 8.1 Antofagasta earthquakes are mostly located over a positive ***Tzz*** signal (Fig. 1) being both events separated by a high gradient signal of more than +10 Eötvös. This region of relative higher ***Tzz*** is coincident with the 1877 seismic gap zone from Metois et al. (2013) shown in Fig. 1. The seismic source of the 2007 Mw = 7.7 Tocopilla earthquake (Fig. 1) is located landwards to this area of relative higher ***Tzz*** values (more than +10 Eötvös). This earthquake shows an anomalous behavior since ruptured only the lower part of the interplate seismogenic zone (Delouis et al., 2009; Béjar-Pizarro et al., 2010; Peyrat et al., 2010; Chlieh et al., 2011) being upwardly limited by an abrupt change in the dip of the interplate seismogenic zone that may have acted as a barrier (Contreras-Reyes et al., 2012). This higher ***Tzz*** signal could be indicating an anomalous region along the seismogenic zone which behaves as a seismic barrier to the propagation of the seismic energy, as proposed by Álvarez et al. (2014).

Even though the main slips of the recent events of Pisagua and Iquique tend to be concentrated over positive ***Tzz*** values, this region presents relative lower values than to the south. The advantage of the availability of the GOCE models, which include data measurements from the last four years before these earthquakes occurred, is making an analysis of the spatial-temporal variations of the gravity field in this region prior to the main rupture (see next section).

5. Discussion

5.1. From GRACE to GOCE

Earth's gravity field temporal variations are mainly due to long-standing mass transfer within the Earth, and at a minor scale depend on other more local phenomena such as mass displacements associated with glacial isostatic adjustments and coseismic redistribution of masses. GRACE (Gravity Recovery and Climate Experiment) data detected earthquake-induced gravity changes over both ocean and land, providing constraints for long-wavelength offshore deformation, from where geodetic

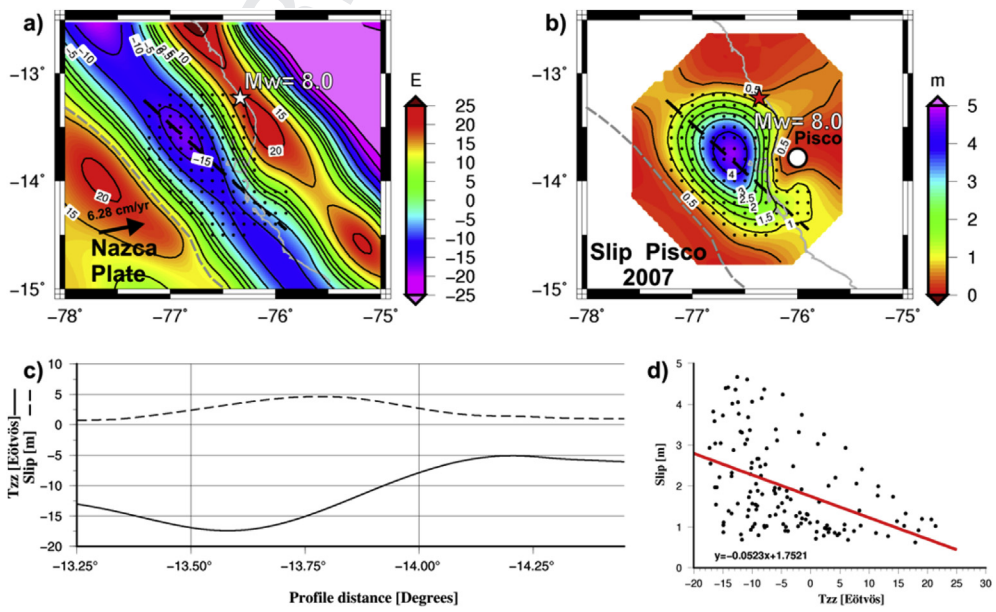

Fig. 2. **Tzz** (a) compared to slip distribution (b) from Chlieh et al. (2011) for the 2007 Mw = 8.0 Pisco event. (c) Profile along **Tzz** vs. Slip and (d) **Tzz** vs. Slip histogram. Note the relationship that exists between low **Tzz** signal and approximate location of the maximum slip. Grey line indicates the coastline, while dashed line indicates the Peru–Chile trench.

Please cite this article in press as: Álvarez, O., et al., Gradients from GOCE reveal gravity changes before Pisagua Mw = 8.2 and Iquique Mw = 7.7 large megathrust earthquakes, Journal of South American Earth Sciences (2015), http://dx.doi.org/10.1016/j.jsames.2015.09.014

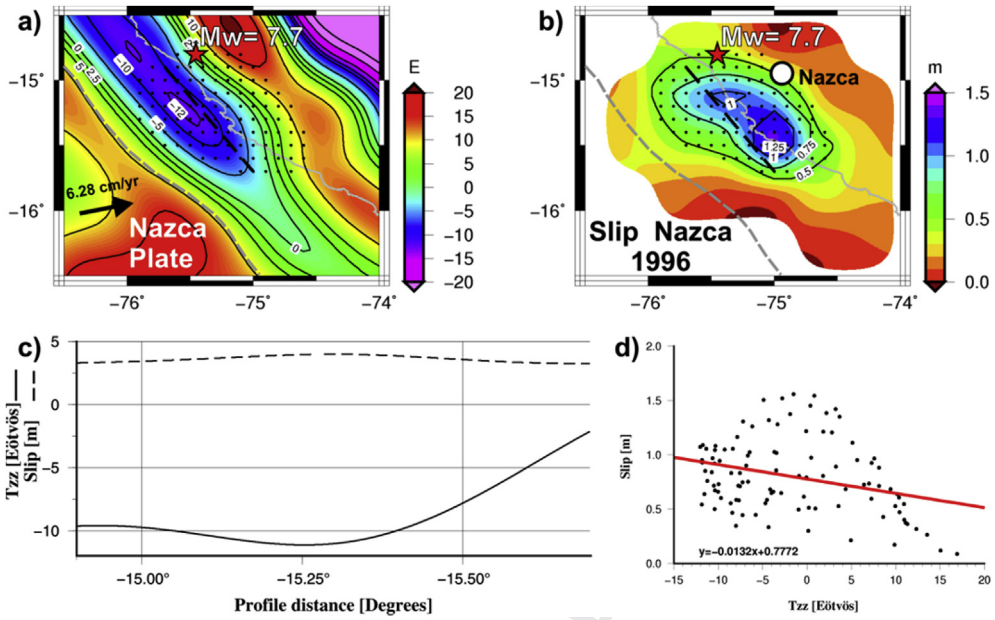

Fig. 3. Tzz (a) compared to slip distribution (b) from Chlieh et al. (2011) for the 1996 Mw = 7.7 Nazca event. (c) Profile along **Tzz** vs. Slip and (d) **Tzz** vs. Slip histogram.

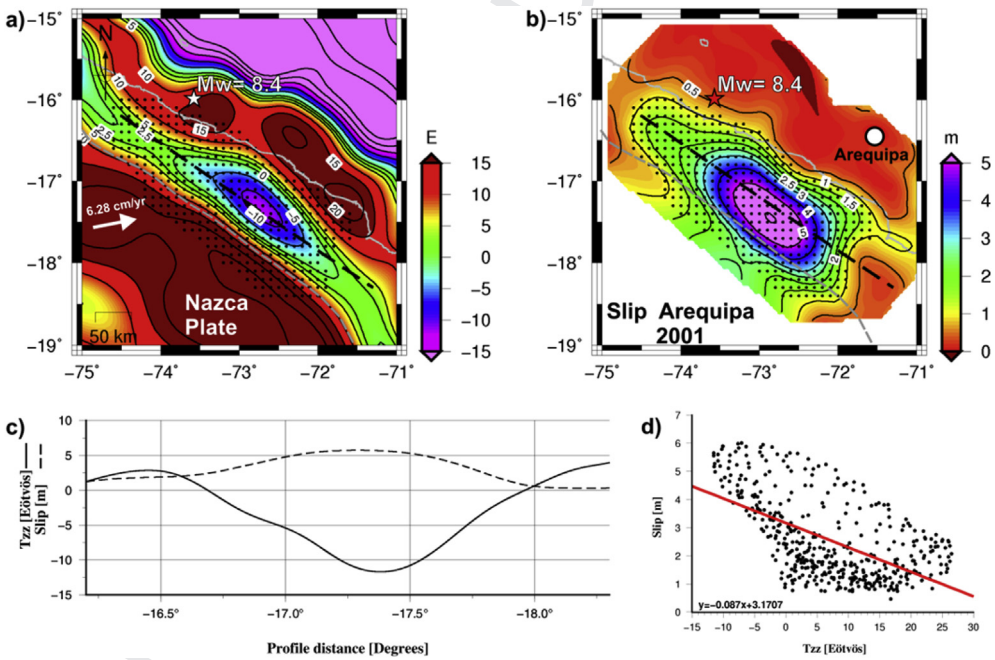

Fig. 4. Tzz (a) compared to slip distribution (b) from Chlieh et al. (2011) for the 2001 Mw = 8.4 Arequipa event. (c) Profile along **Tzz** vs. Slip and (d) **Tzz** vs. Slip histogram.

measurements, such as GPS and InSAR, were not available (Wang et al., 2012). In particular, coseismic variations of the gravity field after the 2004 Mw = 9.2 and 2005 Mw = 8.7 Sumatra earthquakes were detected using a wavelet analysis of GRACE (Tapley et al., 2004) geoids products (Panet et al., 2007). GRACE was also used to detect coseismic and postseismic deformation associated with the Sumatra–Andaman earthquake (Chen et al., 2007). Previously to this, Han et al. (2006) had found an important coseismic gravity decrease in the Andaman Sea that was explained as caused by crustal dilatation after the 2004 earthquake.

Subduction-related earthquakes are in some cases associated with large rupture areas that are expressed by slip distribution models, obtained by a joint inversion of different kind of data (e.g. teleseismic -P, SH and Rayleigh waves-, geodetic -static and continuous GPS, InSAR- and tsunami data). The inversion method (Beresnev, 2003), fault geometry (Lee et al., 2006) and data type (Delouis et al., 2010) influence the determination of the slip distribution. Seismic inversions are also sensitive to the types of included waveform data and the frequency band (Lay et al., 2010; Shao et al., 2010; Pollitz et al., 2011). Page et al. (2009) explained that in regions without enough data constraints, the model would exhibit some artifacts which would look similar to seismic asperities. In this sense, gravity gradients from GOCE are very useful for mapping density related

Please cite this article in press as: Álvarez, O., et al., Gradients from GOCE reveal gravity changes before Pisagua Mw = 8.2 and Iquique Mw = 7.7 large megathrust earthquakes, Journal of South American Earth Sciences (2015), http://dx.doi.org/10.1016/j.jsames.2015.09.014

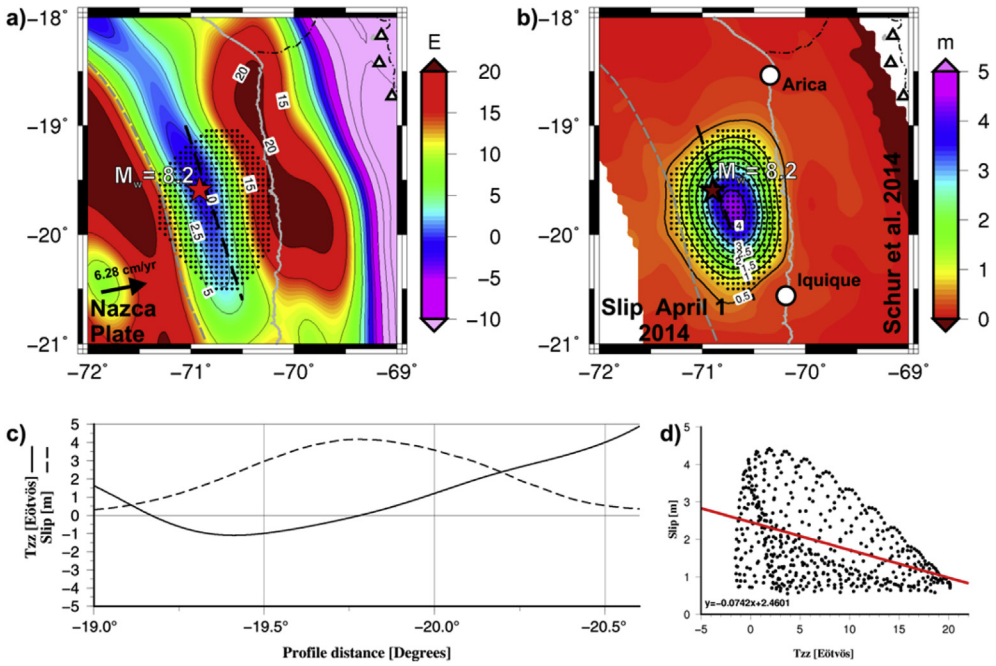

Fig. 5. Tzz (a) compared to slip distribution (b) from Schurr et al. (2014) for the April 01, 2014 Mw = 8.2 Pisagua Earthquake. (c) Profile along **Tzz** vs. Slip and (d) **Tzz** vs. Slip histogram.

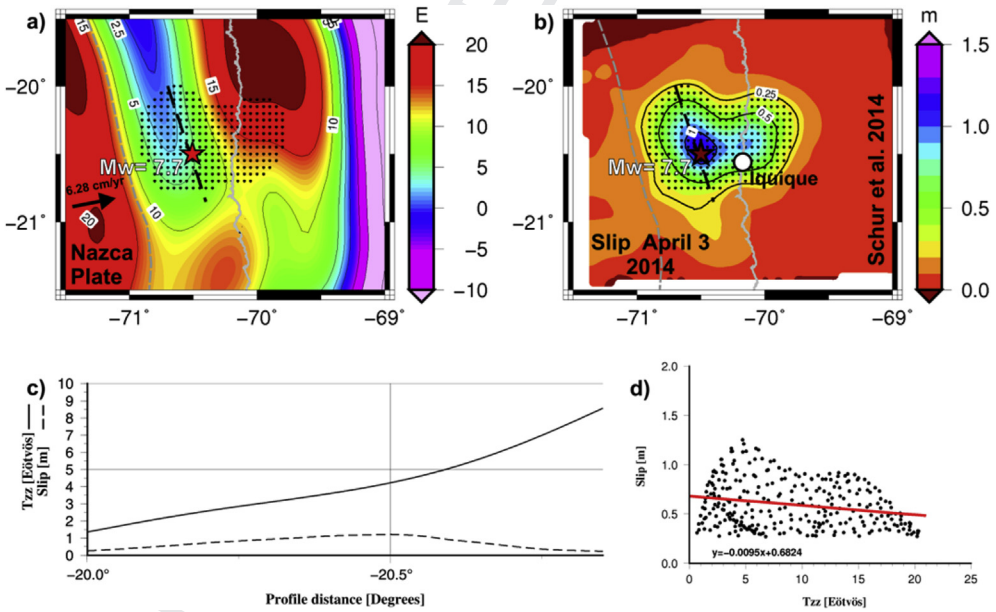

Fig. 6. Tzz (a) compared to slip distribution (b) from Schurr et al. (2014) for the April 03, 2014 Mw 7.7 Iquique earthquake. (c) Profile along **Tzz** vs. Slip and (d) **Tzz** vs. Slip histogram.

heterogeneities since these present a homogeneous coverage and an rather objective tool.

In the Chilean subduction zone, different works (Heki and Matsuo, 2010; Han et al., 2010) have shown the coseismic signature of the 2010 Mw = 8.8 Maule earthquake, by using different methods that led to different resolutions. Unlike the 2004 Sumatra–Andaman earthquake which ruptured a 1500 km-long and 150 km-wide segment along the Sunda subduction zone (Chlieh et al., 2007) leading to more than +10 mGal gravity change in GRACE observation (Han et al., 2006), the 2010 Maule earthquake produced positive gravity changes of only 1–2 mGal which is close to the error level of GRACE observation (Wang et al., 2012).

Even though ESA's GOCE satellite was not designed to visualize changes in Earth's gravity over time, high-resolution gravity gradients of GOCE measured over Antarctica between November 2009 and June 2012 revealed changes in gravity interpreted as associated with a decrease in ice mass volumes. Thus GOCE data complement GRACE data, designed to show changes in Earth gravity field, with a finer resolution. Then, combined datasets have offered a greater insight into the dynamics of the gravity field in many regions (Bouman et al., 2014). For example, signatures in the Earth's gravity field associated with the 2011 Mw = 9.0 Japan Tohoku-Oki

Please cite this article in press as: Álvarez, O., et al., Gradients from GOCE reveal gravity changes before Pisagua Mw = 8.2 and Iquique Mw = 7.7 large megathrust earthquakes, Journal of South American Earth Sciences (2015), http://dx.doi.org/10.1016/j.jsames.2015.09.014

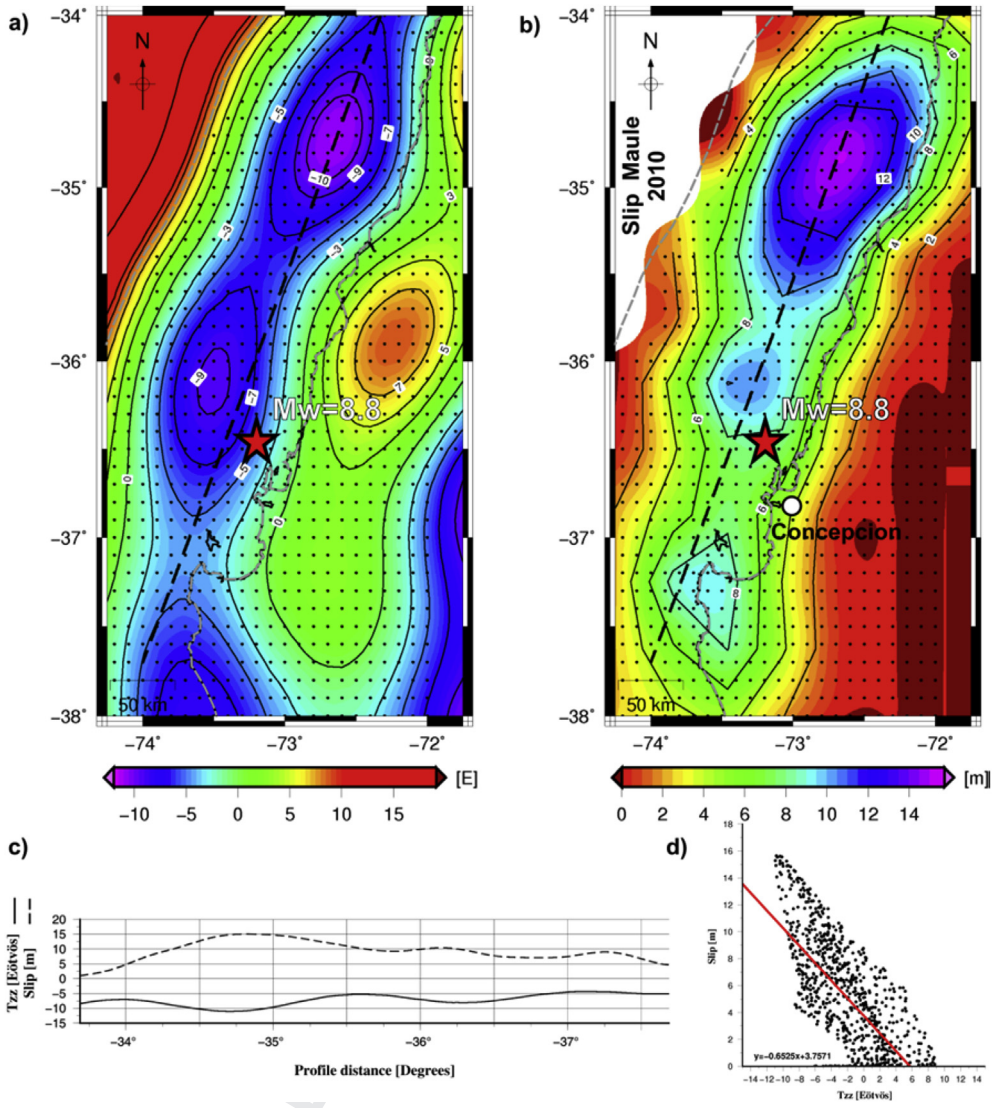

Fig. 7. Tzz (a) compared to slip distribution (b) from Moreno et al. (2012) for the 2010 Mw 8.8 Maule earthquake. (c) Profile along **Tzz** vs. Slip and (d) **Tzz** vs. Slip histogram (modified from Álvarez et al., 2014).

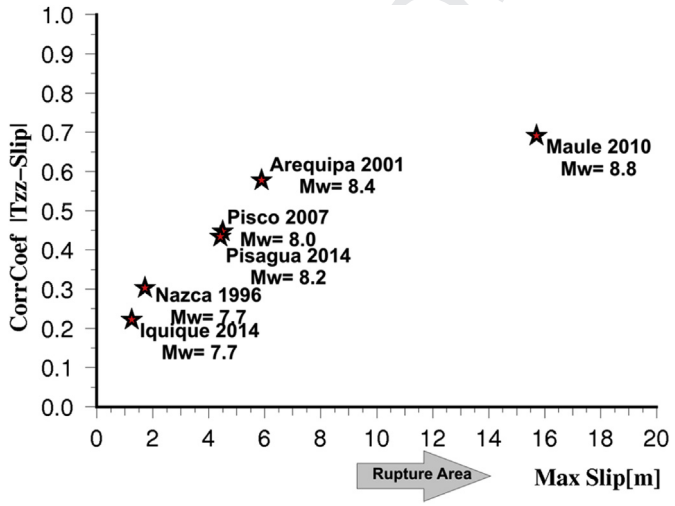

Fig. 8. Correlation coefficient between **Tzz** and Slip versus the maximum slip for different events. As event magnitude increases the correlation between **Tzz** lobes (mGal/m) and high slip (m) increases.

earthquake were detected by data of the GRACE mission but also from the GOCE mission with higher spatial resolution (Fuchs et al., 2013). These authors modeled the coseismic earthquake geoid signal, converting it to vertical gravity gradients at GOCE satellite altitude and thus finding that the earthquake signal is well above the accuracy of the vertical gravity gradients at orbital height. Finally, coseismic gravity changes of the Japan Tohoku-Oki earthquake left a statistically significant signal in the GOCE measured gravity gradients (Fuchs et al., 2013).

Then, the GOCE only models obtained by the Time-wise ***GO_CONS_GCF_2_TIM_R4*** method with an effective data volume of approx. 26.5 months (01/11/2009–19/06/2012) and the ***GO_CONS_GCF_2_TIM_R5*** with an effective data volume of approx. 42 months (data period: 01/11/2009–21/10/2013) constitute good tools for studying the Earth gravity field changes after the 27nd February 2010 Mw = 8.8 Maule and before the April 1st 2014 Mw = 8.2 Pisagua and April 3rd Mw = 7.7 Iquique earthquakes.

Thus, the vertical gravity gradient from ***GO_CONS_GCF_2_TIM_R4*** model (Fig. 9a) was compared to the ***Tzz*** from ***GO_CONS_GCF_2_TIM_R5*** model (Fig. 9b) both calculated up to the same degree/order (N = 250) in the region of the Pisagua and

Please cite this article in press as: Álvarez, O., et al., Gradients from GOCE reveal gravity changes before Pisagua Mw = 8.2 and Iquique Mw = 7.7 large megathrust earthquakes, Journal of South American Earth Sciences (2015), http://dx.doi.org/10.1016/j.jsames.2015.09.014

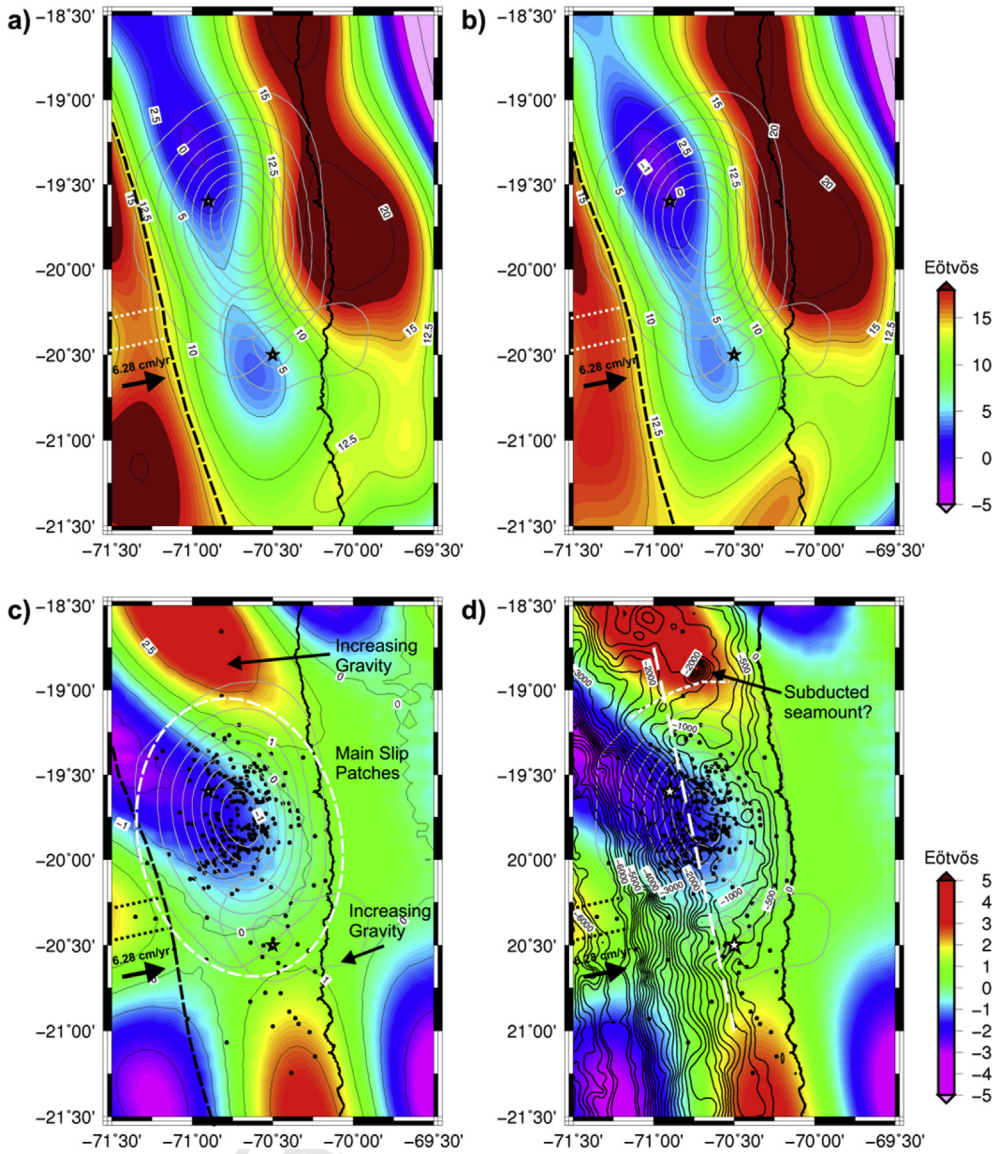

Fig. 9. Topography corrected **Tzz** obtained from **GO_CONS_GCF_2_TIM_R4** (a) and from **GO_CONS_GCF_2_TIM_R5** (b) both up to N = 250. (c) Residual between R5-R4 superimposed to the foreshock sequence (ISC-International Seismological Centre) in the region of the 2014 Mw 8.2 Pisagua and Mw 7.7 Iquique earthquakes, (d) superimposed to the bathymetry from the Digital Elevation Model ETOPO1 (Amante and Eakins, 2009). White dashed line indicates profile of Fig. 10. The white dotted line in (a) shows the segmentation of the outer rise probably related to the subduction of a Hof. Its extrapolation over the seismogenic zone approximately coincides with the relative maximum between both **Tzz** lobes and also with the intersection between both slip models (a and b). The residual between both models (c and d) shows a decrease in the gravity signal over the maximum slip area with two maxima at its northern and southern termination.

Iquique 2014 earthquakes and were superimposed to the main slip distribution of both events (Schurr et al., 2014). The last model shows a decrease in the gravity signal in the region where the maximum slip patch occurred, before the occurrence of the event between 19/6/2012 and 20/10/2013 (Fig. 9c,d). The profile shown in Fig. 10 (center) depicts clearly the negative correlation between residual ***Tzz*** (R5-R4) and Slip distribution for the main shock. North and south of both slip patches an increase in the gravity gradient signal occurred, as it is shown in the residual calculated from both models (Fig. 9c,d and Fig. 10-center). At about 18.8°S, 70.75°W the bathymetry shows a bulk, interpreted as an asperity (subducted seamount?) (Fig. 9d), where the main slip patch ends and the gravity residual computed from models increases (Fig. 9c,d). This is consistent with the relation between subducted Hof's, higher ***Tzz***, and seismic segmentation along the south-central Chilean margin found in other studies (Bilek, 2007; Sparkes et al., 2010; Contreras-Reyes and Carrizo, 2011; Álvarez et al., 2014).

The April 1, 2014 $M_w = 8.2$ earthquake initiated at ~95 km NW of Iquique, at a depth of about 20 km, with both epicenter and focal mechanism consistent with an event that ruptured the plate boundary interface between the Nazca and South America plates. Prior to this earthquake, seismicity rates had increased after March 16 $M_w = 6.7$ event, with similar faulting mechanism. This foreshock sequence (Fig. 9c) had a spatial distribution that migrated to the north, starting near 20°S and moving up to ~19.5°S. This sequence, characterized as a slow slip event (Ruiz et al., 2014; Bürgmann, 2014; Schurr et al., 2014; Moreno et al., 2014; Lay et al., 2014), occurred very close to the region where the vertical gravity gradient signal presents a relative higher amplitude separating a northern main lobe from a southern secondary lobe (Fig. 9a,b). The northern lobe is closer to the main slip patch for the Pisagua event while the

Please cite this article in press as: Álvarez, O., et al., Gradients from GOCE reveal gravity changes before Pisagua Mw = 8.2 and Iquique Mw = 7.7 large megathrust earthquakes, Journal of South American Earth Sciences (2015), http://dx.doi.org/10.1016/j.jsames.2015.09.014

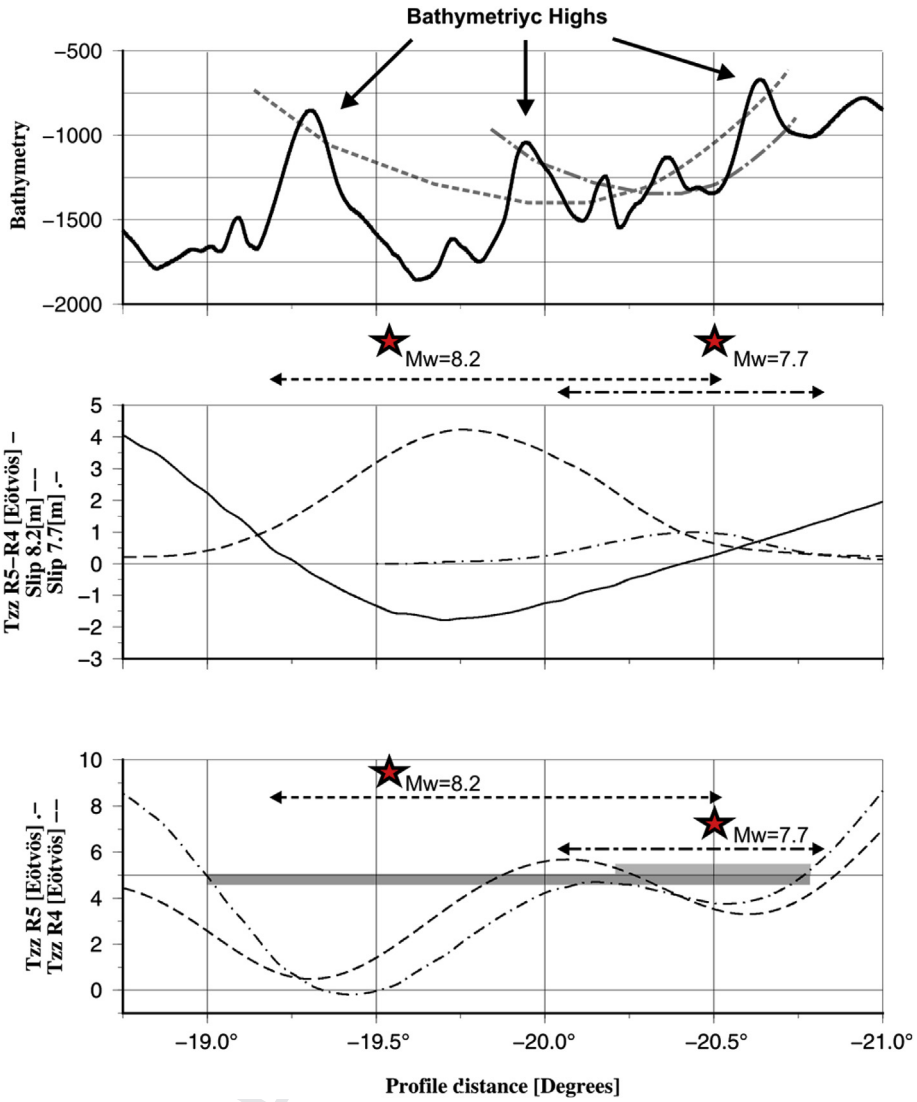

Fig. 10. From top to bottom: Profile along the bathymetry (see location on Fig. 9d) from the Digital Elevation Model ETOPO1 (Amante and Eakins, 2009). Center: Profile along residual **Tzz** between R5-R4 vs. slip distribution for the April 01, 2014 Mw = 8.2 Pisagua and for the April 03, 2014 Mw = 7.7 Iquique earthquakes from Schurr et al. (2014). The negative correlation between residual **Tzz** and Slip is notorious for the main shock. Bottom: **Tzz** from R5 and R4 models (Pail et al., 2011), the relative lower **Tzz** (less than +5 Eötvös, grey shaded) between 19°S to 20.75°S (long wavelength) is well corresponded to the main shock (Mw = 8.2), while the relative lower Tzz between 20.5°S to 20.75°S is related to the main aftershock (Mw = 7.7) The bathymetry (top) also shows a good correspondence with both slip distributions at long wavelength (Dashed line-main shock, Dot and Dashed line-main aftershock).

southern one is related to the Iquique main aftershock, being both separated by an anomaly that segments the outer rise. The relative higher gravity signal between both lobes (R4), and the subsequent gravity fall (R5-R4) could be the expression of upper plate subsidence or extension resulted from basal erosion that could be promoted by a subducting oceanic feature (e.g. seamount, ridge or plateau, dotted line in Fig. 9). The association between forearc basins and slip during subduction thrust earthquakes (Wells et al., 2003) suggests a link between processes controlling upper plate structure and seismic coupling on the subduction-zone thrust fault (Fuller et al., 2006). The last authors, presented a mechanism for the formation of these basins finding that maximum slip during great-thrust earthquakes tends to occur where sedimentary basins stabilize the overlaying wedge, based on numerical simulations. The lack of deformation in these stable regions increases the likelihood of thermal pressurization of the subduction thrust, allows the fault to load faster, and allows greater healing of the fault between rupture events. These effects link deformation of the subduction wedge to the seismic coupling of the subduction thrust (Fuller et al., 2006).

5.1.1. The 2010 Maule event

As previously exposed, both GOCE models cover a data span after the 2010 Mw = 8.8 Maule earthquake. The comparison between both models (Fig. 11a,b) reveals after the event a fall in gravity signal near the trench with an increase towards the coastline. The residual between both models (Fig. 11c) shows that the gravity diminished at a higher rate to the north and south of the main slip patch (between the trench and the +0 Eötvös contour white dashed line in Fig. 11c) probably indicating an increase in the stress accumulation in these regions. Between the +0 Eötvös contour (white dashed line in Fig. 11c) and the coastline, an increase in the gravity residual is observed, probably indicating exhumation of the upper plate due to co-seismic and post-seismic lithospheric stretching along the subduction zone. The area where the main slip occurred (between 34.25°S and 35.5°S) presents a higher residual

Please cite this article in press as: Álvarez, O., et al., Gradients from GOCE reveal gravity changes before Pisagua Mw = 8.2 and Iquique Mw = 7.7 large megathrust earthquakes, Journal of South American Earth Sciences (2015), http://dx.doi.org/10.1016/j.jsames.2015.09.014

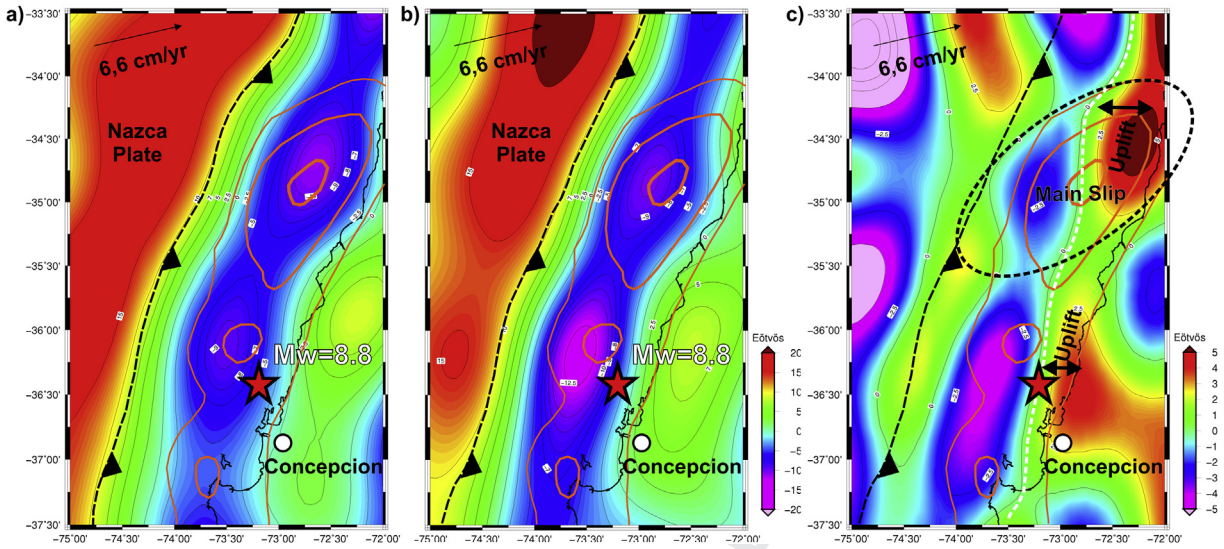

Fig. 11. Topography corrected **Tzz** obtained from **GO_CONS_GCF_2_TIM_R4** (a) and from **GO_CONS_GCF_2_TIM_R5** (b) both up to N = 250. (c) Residual between R5-R4 in the region of the 2010 Mw 8.8 Maule earthquake. The last model shows that the gravity signal decreased at a higher rate in the regions north and south of the maximum slip patch for the data time span between 19/6/2012 and 20/10/2013.

between the +0 Eötvös contour and the coastline, while trenchwards gravity decreased at a lower rate.

5.2. Vertical gravity gradient field and its variations in relation to the earthquake cycle: an indirect measure of the seismic coupling?

The Global Positioning System (GPS) velocity field, acquired between 2008 and 2012 from Metois et al. (2013), describes interseismic deformation between 18°S and 24°S, showing coupling variations on the subduction interface both along-strike and through-dip (Fig 12a). Particularly, they found that the North Chile seismic gap is segmented in at least two highly locked segments where average coupling is higher than the mean value (Loa and Paranal) bounded by narrow areas or intersegment zones of weak coupling (Iquique and Mejillones). The authors related these areas, where average coupling is lower, with high background seismic rate (with both deep intraslab and moderate magnitude subduction-type shallow earthquakes, and post-seismic creep documented for the Mejillones intersegment) to local tectonic complexities on the upper and downgoing plates. These local decreases on the degree of coupling are correlated with structural complexities either in the subducting plate (subduction of a seamount in the Iquique intersegment), or in the upper plate (peninsula crustal-fault system for the Mejillones intersegment) proposing that these zones could either stop or slow down the propagation of seismic ruptures (Metois et al., 2013).

Other studies (Béjar-Pizarro et al., 2013; Metois et al., 2013; Ruiz et al., 2014) indicated stronger coupling on the deeper portion of the megathrust and less coupling updip near the Iquique events on 2014, consistent with the slowly migrating updip foreshock sequence followed by the deeper downdip main shock (Lay et al., 2014). Lay et al. (2014) proposed that improved onshore and offshore geodetic and seismic networks in many regions are needed to establish the role of slow-slip events in foreshock sequences and to have a better confidence in the identification of foreshock sequences prior to large interplate events.

GOCE models present homogeneous quality of data (both onshore and offshore) overcoming the lack of data present in other methods and thus being a good tool for mapping crustal heterogeneities. Structural complexities either in the subducting plate or in the upper plate were correlated with a local decrease in the degree of coupling (Metois et al., 2013), so we compared the ***Tzz*** (Fig. 12b) from the model ***GO_CONS_GCF_2_TIM_R4*** up to N = 250 (it integrates data acquired between 2009 and 2012) to the seismic coupling (Fig. 12a) based on a GPS data span between 2008 and 2012 (Metois et al., 2013; Ruiz et al., 2014). We found over the seismogenic zone a spatial correlation between the different segments and intersegments proposed by Metois et al. (2013), relating a higher coupling degree to higher ***Tzz*** values (Fig. 12a,b).

Holtkamp and Brudzinski (2011) found that certain earthquake swarms localized around the Pacific subduction zones tended to concentrate in regions of either low interplate coupling or on the margins of large slip zones as it is the case for the Iquique earthquakes. Gravity changes before the occurrence of both megathrust earthquakes reveal a decrease in ***Tzz*** over the region where the foreshocks occurred (Fig. 9c,d). Thus, as the coupling coefficient could be considered as a proxy for the mechanical behavior of the subduction interface (Metois et al., 2013), gravity field variations (revealing changes in density structure across the interplate) could be indirectly related to variations in stress coupling. Variations in the ***Tzz*** $\left(Tzz = \frac{\partial^2 T}{\partial r^2}\right)$ are related to gravity changes in the radial direction so it could be a good indicator of mass redistribution before and after a megathrust event, and also with vertical stress variations ($\sigma_{zz} = \rho g z$).

5.3. Correlation between Tzz and seismic b-value

The slope in the Gutenberg–Richter relation (Gutenberg and Richter, 1944; Ishimoto and Iida, 1939) which relates the frequency of earthquake occurrence and the magnitudes of earthquakes in a certain area is represented by the seismic *b-value*. It has been commonly used to describe statistically the relative occurrence of large and small events (a high *b-value* indicates a larger proportion of small earthquakes, and vice versa for a specific area) (Schorlemmer et al., 2005). In seismically active regions the long-term average *b-value* is close to unity, although a wider ranging of possible values ($0.3 \leq b \leq 2.5$) has been reported in the literature (El-Isa and Eaton, 2014). The *b-value* varies systematically for different styles of deformation, being normal faulting events

Please cite this article in press as: Álvarez, O., et al., Gradients from GOCE reveal gravity changes before Pisagua Mw = 8.2 and Iquique Mw = 7.7 large megathrust earthquakes, Journal of South American Earth Sciences (2015), http://dx.doi.org/10.1016/j.jsames.2015.09.014

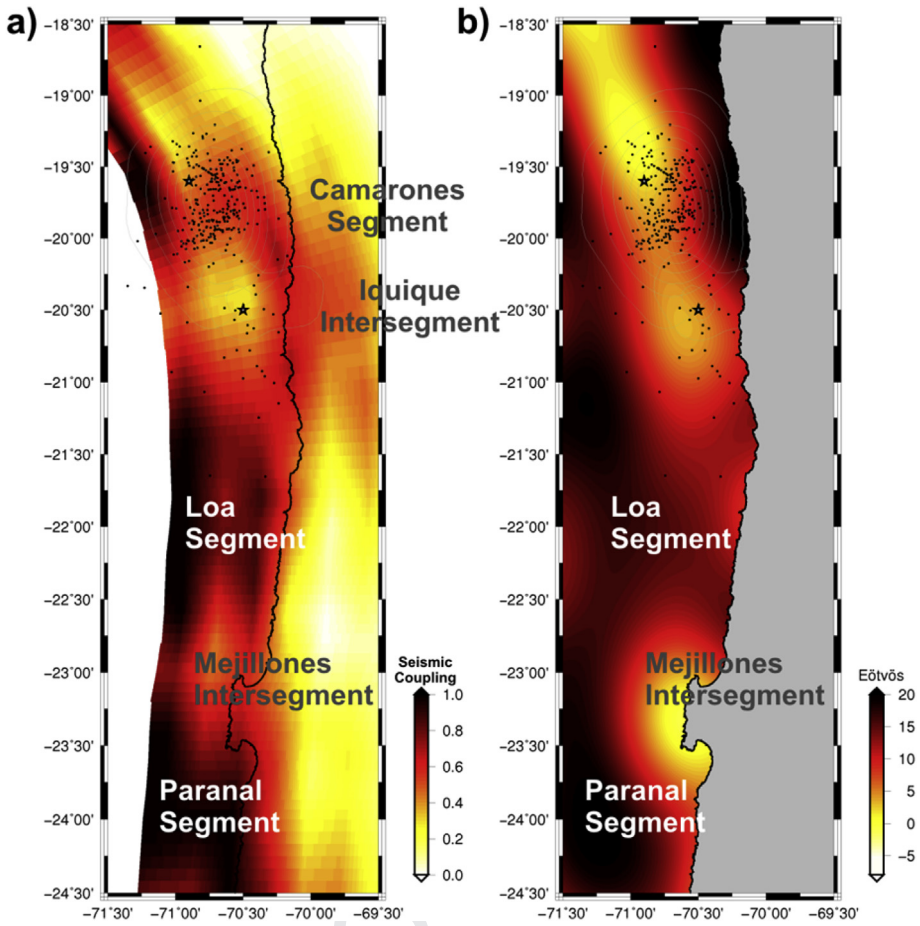

Fig. 12. (a) Seismic coupling from Ruiz et al. (2014), the different segments were defined by Metois et al. (2013) based on differences in degree of coupling. (b) topography corrected **Tzz** from the **GO_CONS_GCF_2_TIM_R4** up to N = 250. A good correspondence between the different segments is observed over the seismogenic zone.

usually characterized by higher *b*-values, while events associated with contractional settings tend to present lower values (Schorlemmer et al., 2005). This variability is also sensitive to a variety of other factors such as prevailing stress state, crustal heterogeneities, focal depth, pore pressure, geothermal gradient, tectonic setting, petrological/environmental/geophysical characteristics, clustering of events, incomplete catalog data, and/or method, factors that seem to be linked, directly or indirectly, to the effective state of stress (El-Isa and Eaton, 2014). Schorlemmer et al. (2005) inferred that the *b*-value acts as a stress meter that depends inversely on differential stress. Ghosh et al. (2008) proposed that b-*value* studies may be useful in identifying regions of increased interface locking in subduction zones, which may indicate regions capable of large slip in future large earthquakes after examining seismicity patterns across Nicoya, Costa Rica. Similar to the 2009 l'Aquila earthquake (De Gori et al., 2012), the foreshock activity for the Iquique events occurred close to a low b-value zone (Schurr et al., 2014).

Sobiesiak et al. (2007) observed positive correlations between seismic *b-value*, isostatic residual gravity anomalies (IR) and geologic structures south of the Mejillones peninsula (from 23°S to 24.4°S, Fig. 5 of Sobiesiak et al., 2007). The isostatic corrections are used to remove, in part, the effect of the crustal roots or deeper masses from the gravity anomalies, allowing to highlight geological structures located in the upper crust. Thus, the isostatic residual anomaly (Cordell et al., 1991) is a method to highlight gravity anomalies in the upper crust which gives very similar results to the vertical gravity gradient. We mapped (Fig. 13a) the seismic *b-value* from Schurr et al. (2014) north of the Mejillones peninsula (−23°S to −19°S) over the seismogenic zone and compared it to the topography and sediment corrected ***Tzz*,** finding a good correlation between both quantities. The study of Wyss et al. (2004) in the Parkfield and Morgan Hill sections of the San Andreas fault system supports the hypothesis that low *b-values* prior to a large earthquake indicate position of asperities on the fault plane.

Different case studies (Wyss and Lee, 1973; Smith, 1981, 1986; Li et al., 1978; Imoto, 1991; Hirose et al., 2002; Tsukakoshi and Shimazaki, 2008; Schurr et al., 2014) show a tendency for the *b-value* to decrease prior to a large earthquake, and that in a high stress state, the seismic *b-value* decreases particularly in the region where maximum slip occurs. This decrease in *b-value* prior to large earthquakes has been confirmed in numerical simulations (Yamashita and Knopoff, 1992; Hainzl et al., 2003) and also in laboratory experiments (Scholz, 1968; Ohnaka and Mogi, 1982; Sammonds et al., 1992; Lei et al., 2004).

Considering the positive correlation between the ***Tzz*** and *b-value* (Fig. 13) and also with IR (Sobiesiak et al., 2007), we can use gravity as an indirect tool for mapping low *b-value* zones and more indirectly potential zones of asperities along the seismogenic zone that could trigger large events (Álvarez et al., 2014). Particularly, taking into account the decrease of the gravity signal in the region where maximum slip occurred prior to the Iquique events (Fig. 9c), we can relate it (Fig. 13c) to the decrease in the *b-value* reported for several events including the analyzed ones. Regarding to this, a

Please cite this article in press as: Álvarez, O., et al., Gradients from GOCE reveal gravity changes before Pisagua Mw = 8.2 and Iquique Mw = 7.7 large megathrust earthquakes, Journal of South American Earth Sciences (2015), http://dx.doi.org/10.1016/j.jsames.2015.09.014

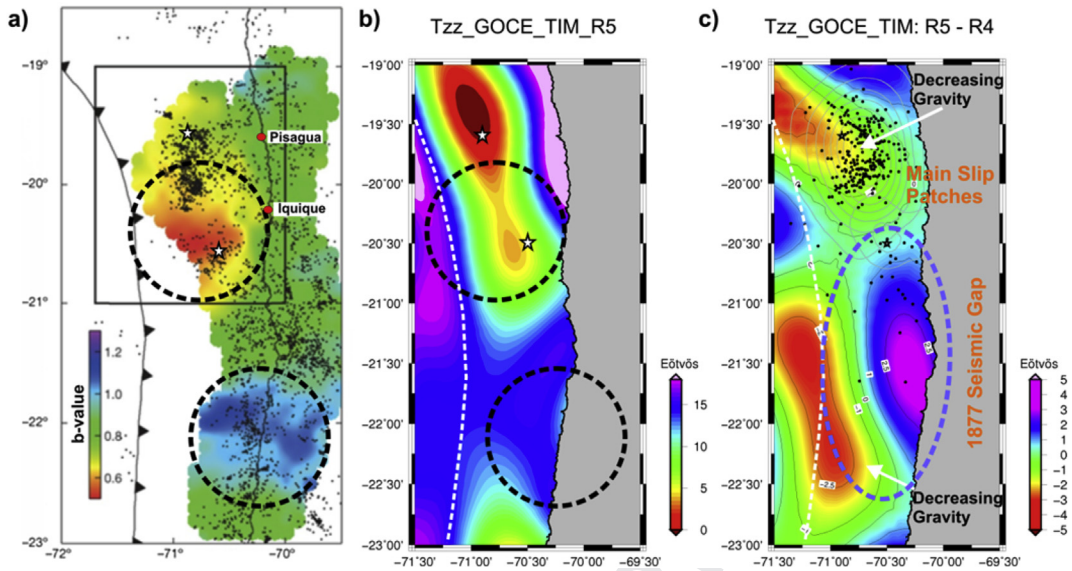

Fig. 13. (a) b-value (Fig. 12a) from Schurr et al. (2014), (b) topography corrected **Tzz** from the **GO_CONS_GCF_2_TIM_R5** up to N = 250. (c) Residual between R5-R4 models superimposed to the foreshock sequence (ISC-International Seismological Centre) in the region of the 2014 Mw 8.2 Pisagua and Mw 7.7 Iquique earthquakes. It is proposed that the fall in gravity signal could be related to a decrease in b-value.

decrease in the gravity signal is also observed in the region of the 1877 seismic gap. But in this case, the gravity decrease fills only the trench-wards half of the seismogenic zone (Fig. 13c). To the north, were the Piasgua and Iquique events occurred, the gravity decrease filled the entire seismogenic zone between the trench and the coastline. If subsequent gravity models show that this decrease in gravity over the 1877 seismic gap advances landwards, it should be considered as a potential increase of the probable occurrence of a great megathrust event in the region.

6. Conclusions

Satellite gravimetry has been used to detect earthquake-induced gravity changes, with the advantage of presenting homogeneous data coverage and increasing precision between different missions. As previously noted for the south Central Chilean margin, high ***Tzz*** values interposed between the trench and the coastline coincide with the extent of the recognized rupture zones of recent earthquakes. On the other hand maximum slips into rupture zones of large megathrust earthquakes in northern Chile and southern Peru are concentrated near low ***Tzz*** values. This relationship is particularly clear for those events with Mw $\geq$ 8.0, probably due to the high wavelength characteristic of the gravity derived signal.

From the comparison between the Tzz derived from the two last satellite GOCE only models ***GO_CONS_GCF_2_TIM_R4*** and ***GO_CONS_GCF_2_TIM_R5***, we propose that temporal variations in the gravity field are probably related to mass redistribution-changes or variations in fluid pressure after and before the 2010 Mw = 8.8 Maule and the 2014 Mw = 8.2 Pisagua earthquakes respectively. Regarding this, we found a good agreement between the main slip patch for the last earthquake and its main shock with a gravity fall and an increase at its northern and southern terminations. Moreover the gravity signal presents a relative higher value close to the area of the foreshocks, probably indicating the presence of an asperity. These HOF's have been related to increases in the seismic activity with low magnitude and basal erosion of the upper plate in the region where the plate interaction occurs. This mechanism could explain the foreshock sequence and the gravity fall at least in the last two years prior to the main shock of April 1st 2014. This gravity fall is probably related to upper plate collapse and extension due to the basal erosion (Fig. 9b).

When comparing both models for the 2010 Mw = 8.8 Maule event, we found a gravity decrease near the trench, but this fall is higher north and south of the main slip patch, probably indicating a higher rate of gravity diminution due to an increase in the stress in these regions, were the slip was minor. Towards the coastline the gravity derived signal indicates an increase probably related to the uplift along the coast after the Maule event.

Vertical gravity gradient derived from satellite GOCE is an important quantity for delineating structural heterogeneities related to density changes both in the upper and downgoing plates, and for analyzing the different phenomena related to the subduction of high oceanic features such as seamounts, plateaus and ridges. These oceanic features could act as seismic barriers (Fig. 9d) when are related to a high gravity signal and also promote earthquakes by upper plate erosion and subsequent extensional collapse, shown by lows and/or a decrease in the gravity signal. Moreover important relationships between ***Tzz*** and other quantities such as seismic *b-value* and even seismic coupling need to be explored in more detail. This analysis suggests that the GOCE only model, and in particular the calculation of the second spatial derivative of the anomalous potential T in the radial direction (***Tzz***), could be used as a predictive tool to determine potential coseismic displacements in a seismic gap, such as the case study of the Iquique gap in northern Chile. The advantages of gravity satellite derived data are the homogeneous coverage over the whole plate interface, and that data are available before the earthquake occurrence. This study highlights the importance of further improvements in the monitoring of spatio-temporal variations in the earth gravity field at interplate regions through satellite gravity missions.

Acknowledgments

Authors acknowledge the use of the GMT-mapping software of Wessel and Smith (1998) and to Dr. Gavin P. Hayes, Research Geophysicist at USGS National Earthquake Information Center for his useful preliminar slip models and helpfull and constructive comments. Thanks to the Abdus Salam ICTP for covering the full

Please cite this article in press as: Álvarez, O., et al., Gradients from GOCE reveal gravity changes before Pisagua Mw = 8.2 and Iquique Mw = 7.7 large megathrust earthquakes, Journal of South American Earth Sciences (2015), http://dx.doi.org/10.1016/j.jsames.2015.09.014

trip and expenses for attending the Advanced workshop and school of great megathrust earthquakes and tsunamis held at Grignano-Trieste, Italy, and for the helpfull and constructive comments to Dr. T. Lay, Dr. B. Schurr, Dr. M. Metois and Dr. A. Auodia. The authors would like to thank to CONICET and the Ministerio de Ciencia y Técnica - Agencia de Promoción Científica y Tecnológica, PICT07-1903 for financial support.

References

Adam, J., Reuther, C.D., 2000. Crustal dynamics and active fault mechanics during subduction erosion. Application of frictional wedge analysis on to the North Chilean forearc. Tectonophysics 321, 297–325.

Alvarez, O., Gimenez, M.E., Braitenberg, C., Folguera, A., 2012. GOCE satellite derived gravity and gravity gradient corrected for topographic effect in the South Central Andes region. Geophys. J. Int. 190 (2), 941–959. http://dx.doi.org/10.1111/j.1365-246X.2012.05556.x.

Alvarez, O., Gimenez, M.E., Braitenberg, C., 2013. Nueva metodología para el cálculo del efecto topográfico para la corrección de datos satelitales. Rev. Asoc. Geol. Arg. 70 (4), 422–429.

Álvarez, O., Nacif, S., Gimenez, M., Folguera, A., Braitenberg, A., 2014. Goce derived vertical gravity gradient delineates great earthquake rupture zones along the Chilean margin. Tectonophysics 622, 198–215. http://dx.doi.org10.1016/j.tecto.2014.03.011.

Alvarez, O., Gimenez, M.E., Martinez, M.P., LinceKlinger, F., Braitenberg, C., 2015a. New insights into the Andean crustal structure between 32° and 34°S from GOCE satellite gravity data and EGM2008 model. In: Sepúlveda, S.A., Giambiagi, L.B., Moreiras, S.M., Pinto, L., Tunik, M., Hoke, G.D., Farías, M. (Eds.), Geodynamic Processes in the Andes of Central Chile and Argentina, vol. 399. Geological Society, London, pp. 183–202. Special Publications. http://dx.doi.org/10.1144/SP399.3.

Alvarez, O., Gimenez, M., Folguera, A., Spagnotto, S., Bustos, E., Baez, W., Braitenberg, C., 2015b. New evidence about the subduction of the Copiapó ridge beneath South America, and its connection with the Chilean-Pampean flat slab, tracked by satellite GOCE and EGM2008 models. J. Geodyn. (in press) http://dx.doi.org/10.1016/j.jog.2015.08.002.

Amante, C., Eakins, B.W., 2009. ETOPO1, 1 Arc-Minute Global Relief Model: Procedures, Data Sources and Analysis. NOAA Technical Memorandum NESDIS NGDC-24, p. 19. March 2009.

Bangs, N.L., Cande, S.C., 1997. Episodic development of a convergent margin inferred from structures and processes along the southern Chile margin. Tectonics 16 (3), 489–505.

Barthelmes, F., 2009. Definition of functionals of the geopotential and their calculation from spherical harmonic models. Scientific Technical Report, STR09/02. In: Theory and Formulas Used by the Calculation Service of the International Centre for Global Earth Models (ICGEM). GFZ German Research Centre for Geosciences, Postdam, Germany. World Wide Web Address. http://icgem.gfz-postdam.de.

Béjar-Pizarro, M., Carrizo, D., Socquet, A., Armijo, R., Barrientos, S., Bondoux, F., Bonvalot, S., Campos, J., Comte, D., de Chabalier, J.B., Charade, O., Delorme, A., Gabalda, G., Galetzka, J., Genrich, J., Nercessian, A., Olcay, M., Ortega, F., Ortega, I., Remy, D., Ruegg, J.C., Simons, M., Valderas, C., Vigny, C., 2010. Asperities and barriers on the seismogenic zone in north Chile: state-of-the-art after the 2007 Mw 7.7 Tocopilla earthquake inferred by GPS and InSAR data. Geophys. J. Int. 183, 390–406. http://dx.doi.org/10.1111/j.1365-246X.2010.04748.x.

Beresnev, I.A., 2003. Uncertainties in finite-fault slip inversions: to what extent to believe? (A critical review). Bull. Seismol. Soc. Am. 93, 2445–2458.

Bilek, S.L., 2007. Influence of subducting topography on earthquake rupture. In: Dixon, T., Moore, C. (Eds.), The Seismogenic Zone of Subduction Thrust Faults. Columbia University Press, pp. 123–146.

Bouman, J., Ebbing, J., Fuchs, M., 2013. Reference frame transformation of satellite gravity gradients and topographic mass reduction. J. Geophys. Res. Solid Earth 118 (2), 759–774. http://dx.doi.org/10.1029/2012JB009747.

Bouman, J., Fuchs, M., Ivins, E., van der Wal, W., Schrama, E., Visser, P., Horwath, M., 2014. Antarctic outlet glacier mass change resolved at basin scale from satellite gravity gradiometry. Geophys. Res. Lett. 41 (16), 5919. http://dx.doi.org/10.1002/2014GL060637.

Braitenberg, C., Mariani, P., Ebbing, J., Sprlak, M., 2011. The enigmatic Chad lineament revisited with global gravity and gravity-gradient fields. In: Van Hinsbergen, D.J.J., Buiter, S.J.H., Torsvik, T.H., Gaina, C., Webb, S.J. (Eds.), The Formation and Evolution of Africa: a Synopsis of 3.8 Ga of Earth History, Geol. Soc. Lond. Spec. Publ., vol. 357. Geological Society, London, pp. 329–341. http://dx.doi.org/10.1144/SP357.18.

Brockmann, J.M., Zehentner, N., Höck, E., Pail, R., Loth, I., Mayer-Gürr, T., Schuh, W.D., 2014. EGM_TIM_RL05: an independent geoid with centimeter accuracy purely based on the GOCE mission. Geophys. Res. Lett. 41, 8089–8099.

Bürgmann, R., 2014. Warning signs of the Iquique earthquake. Nature 512, 258–259.

Chen, J.L., Wilson, C.R., Tapley, B.D., Grand, S., 2007. GRACE detects coseismic and postseismic deformation from the Sumatra–Andaman earthquake. Geophys. Res. Lett. 34, L13302.

Chlieh, M., de Chabalier, J.B., Ruegg, J.C., Armijo, R., Dmowska, R., Campos, J., Feigl, K.L., 2004. Crustal deformation and fault slip during the seismic cycle in the North Chile subduction zone, from GPS and InSAR observations. Geophys. J. Int. 158 (2), 695–711.

Chlieh, M., Avouac, J.P., Hjorleifsdottir, V., Song, T.R.A., Ji, C., Sieh, K., Sladen, A., Hebert, H., Prawirodirdjo, L., Bock, Y., Galetzka, J., 2007. Coseismic slip and afterslip of the great Mw 9.15 Sumatra–Andaman earthquake of 2004. Bull. Seismol. Soc. Am. 97, S152–S173.

Chlieh, M., Perfettini, H., Tavera, H., Avouac, J., Remy, D., Nocquet, J., Rolandone, F., Bondoux, F., Gabalda, G., Bonvalot, S., 2011. Interseismic coupling and seismic potential along the Central Andes subduction zone. J. Geophys. Res. 116, B12405. http://dx.doi.org/10.1029/2010JB008166.

Comte, D., Pardo, M., 1991. Reappraisal of great historical earthquakes in the Northern Chile and Southern Peru Seismic Gaps. Nat. Hazards 4, 23–44.

Contreras-Reyes, E., Carrizo, D., 2011. Control of high oceanic features ans subduction channel on earthquake ruptures along the Chile-Peru subduction zone. Phys. Earth Planet. Int. 186, 49–58.

Contreras-Reyes, E., Jara, J., Grevemeyer, I., Ruiz, S., Carrizo, D., 2012. Abrupt change in the dip of the subducting plate beneath north Chile. Nat. Geosci. 5, 342–345. http://dx.doi.org/10.1038/ngeo1447.

Cordell, L., Zorin, Y.A., Keller, G.R., 1991. The decompensative gravity anomaly and deep structure of the region of the Rio Grande rift. J. Geophys. Res. 96, 6557–6568.

De Gori, P., Lucente, F.P., Lombardi, A.M., Chiarabba, C., Montuori, C., 2012. Heterogeneities along the 2009 l'Aquila fault inferred by the b-value distribution. Geophys. Res. Lett. 39, L15304. http://dx.doi.org/10.1029/2012GL052822.

Delouis, B., Nocquet, J., Vallée, M., 2010. Slip distribution of the February 27, 2010 Mw = 8.8 Maule earthquake, central Chile, from static and high-rate GPS, InSAR, and broadband teleseismic data. Geophys. Res. Lett. 37 http://dx.doi.org/10.1029/2010GL043899.

Delouis, B., Pardo, M., Legrand, D., Monfret, T., 2009. The Mw 7.7 Tocopilla earthquake of 14 November 2007 at the southern edge of the northern Chile seismic gap: rupture in the deep part of the coupled plate interface. Bull. Seismol. Soc. Am. 99 (1), 87–94. http://dx.doi.org/10.1785/0120080192.

Divins, D.L., 2003. Total Sediment Thickness of the World's Oceans and Marginal Seas. NOAA National Geophysical Data Center, Boulder, CO.

Dorbath, L., Cisternas, A., Dorbath, C., 1990. Quantitative assessment of great earthquakes in Peru. Bull. Seismol. Soc. Am. 80, 551–576.

Dreger, D., Kaverina, A., 2000. Seismic remote sensing for the earthquake source process and near-source strong shaking: a case study of the October 16, 1999 Hector Mine earthquake. Geophys. Res. Lett. 27 (13), 1941–1944.

El-Isa, Z.H., Eaton, D.W., 2014. Spatiotemporal variations in the b-value of earthquake magnitude–frequency distributions: classification and causes. Tectonophysics 615–616, 1–11.

Fuller, C.W., Willett, S.D., Brandon, M.T., 2006. Formation of forearc basins and their influence on subduction zone earthquakes. Geology 34 (2), 65–68. http://dx.doi.org/10.1130/G21828.1, 0.

Fuchs, M.J., Bouman, J., Broerse, T., Visser, P., Vermeersen, B., 2013. Observing coseismic gravity change from the Japan Tohoku-Oki 2011earthquake with GOCE gravity gradiometry. J. Geophys. Res. 118, 5712–5721. http://dx.doi.org/10.1002/jgrb.50381.

Garzione, C., Hoke, G., Libarkin, J., Withers, S., MacFadden, B., Eiler, J., Ghosh, P., Mulch, A., 2008. Rise of the Andes. Science 320, 1304. http://dx.doi.org/10.1126/science.1148615.

Ghosh, A., Newman, A.V., Thomas, A.M., Farmer, G.T., 2008. Interface Locking along the Subduction Megathrust from b-value Mapping Near Nicoya Peninsula, 35. Geophys. Res. Lett., Costa Rica, p. L01301. http://dx.doi.org/10.1029/2007GL031617.

Grombein, T., Heck, B., Seitz, K., 2013. Optimized formulas for the gravitational field of a tesseroid. J. Geod. 87, 645–660.

Gutenberg, R., Richter, C.F., 1944. Frequency of earthquakes in California. Bull. Seismol. Soc. Am. 34, 185–188.

Hainzl, S., Zoller, G., Kurths, J., 2003. Earthquake clusters resulting from delayed rupture propagation in finite fault segments. J. Geophys. Res. 108 (B1) http://dx.doi.org/10.1029/2001JB000610.

Han, S.C., Sauber, J., Luthcke, S., 2010. Regional gravity decrease after the 2010 Maule (Chile) earthquake indicates large-scale mass redistribution. Geophys. Res. Lett. 37, L23307.

Han, S.C., Shum, C.K., Bevis, M., Ji, C., Kuo, C.Y., 2006. Crustal dilatation observed by GRACE after the 2004 Sumatra–Andaman earthquake. Science 313 (5787), 658–666.

Hartley, A.J., Jolley, E.J., 1995. Tectonic implications of late Cenozoic sedimentation from the coastal Cordillera of northern Chile (22–24°S). J. Geol. Soc. Lond. 152, 51–63.

Haschke, M., Günther, A., Melnick, D., Echtler, H., Reutter, K., Scheuber, E., Oncken, O., 2006. Central and southern andean tectonic evolution inferred from arc magmatism. Frontiers in Earth Sciences. In: Oncken, O., Chong, G., Franz, G., Giese, P., Götze, H.J., Ramos, V., Strecker, M., Wigger, P. (Eds.), The Andes – Active Subduction Orogeny. Springer, pp. 337–353. http://dx.doi.org/10.1007/978-3-540-48684-8, 16.

Hayes, G.P., Herman, M.W., Barnhart, W.D., Furlong, K.P., Riquelme, S., Benz, H.M., Bergman, E., Barrientos, S., Earle, P.S., Samsonov, P., 2014. Continuing megathrust earthquake potential in Chile after the 2014 Iquique earthquake. Nature 512, 295–298. http://dx.doi.org/10.1038/nature13677.

Heck, B., Seitz, K., 2007. A comparison of the tesseroid, prism and point mass

approaches for mass reductions in gravity field modeling. J. Geod. 81 (2), 121–136. http://dx.doi.org/10.1007/s00190-006-0094-0.
Heki, K., Matsuo, K., 2010. Coseismic gravity changes of the 2010 earthquake in central Chile from satellite gravimetry. Geophys. Res. Lett. 37, L24306.
Hirose, F., Nakamura, A., Hasegawa, A., 2002. b-value variation associated with the rupture of asperities – spatial and temporal distributions of b-value East off NE Japan. Zisin II 55, 249–260 (in Japanese).
Holtkamp, S., Brudzinski, M.R., 2011. Circum pacific earthquake swarms. Earth Planet. Sci. Lett. 305, 215–225. http://dx.doi.org/10.1016/j.epsl.2011.03.004.
Hofmann-Wellenhof, B., Moritz, H., 2006. Phys. Geod., second ed. Springer, Berlin, p. 286.
Imoto, M., 1991. Changes in the magnitude-frequency b-value prior to large (M = 6.0) earthquakes in Japan. Tectonophysics 193, 311–325.
Ishimoto, M., Iida, K., 1939. Observations of earthquakes registered with the microseismograph constructed recently. Bull. Earthq. Res. Inst. 17, 443–478.
Janak, J., Sprlak, M., 2006. New software for gravity field modelling using spherical armonic. Geod. Cartog. Hor. 52, 1–8 (in Slovak).
Kausel, E., 1986. Los terremotos de agosto de 1868 y mayo de 1877 que afectaron el sur del PeŠŕu y norte de Chile. Bol. Acad. Chil. Cienc. 3, 8–14.
Kay, S., Godoy, E., Kurtz, A., 2005. Episodic arc migration, crustal thickening subduction erosion and magmatism in the south-central Andes. Bull. Geol. Soc. Am. 117, 67–88.
Kelleher, J.A., 1972. Rupture zones of large South American earthquakes and some predictions. J. Geophys. Res. 77, 2087–2103.
Kendrick, E., Bevis, M., Smalley, R., Brooks, B., Barriga, R., Lauri, E., 2003. The Nazca – south america Euler vector and its rate of change. J. South Am. Earth Sci. 16, 125–131.
Lamb, S., Davis, P., 2003. Cenozoic climate change as a possible cause for the rise of the Andes. Nature 425, 792–797.
Lay, T., Ammon, C.J., Kanamori, H., Koper, K.D., Sufri, O., Hutko, A.R., 2010. Teleseismic inversion for rupture process of the 27 February 2010 Chile (Mw=8.8) earthquake. Geophys. Res. Lett. 37, L1330 1. http://dx.doi.org/10.1029/2010GL043379.
Lay, T., Yue, H., Brodsky, E.E., An, C., 2014. The 1 April 2014 Iquique, Chile, Mw 8.1 earthquake rupture sequence. Geophys. Res. Lett. 41, 3818–3825. http://dx.doi.org/10.1002/2014GL060238.
Lee, S.H., Ma, K.F., Chen, H.W., 2006. Effects of fault geometry and slip style on near-fault static displacements caused by the 1999 Chi-Chi, Taiwan earthquake. Earth Planet. Sci. Lett. 241 (1–2), 336–350.
Lei, X.L., Masuda, K., Nishizawa, O., Jouniaux, L., Liu, L., Ma, W., Satoh, T., Kusunose, K., 2004. Detailed analysis of acoustic emission activity during catastrophic fracture of faults in rocks. J. Struct. Geol. 26, 247–258.
Li, Q., Cen, J., Yu, L., Hao, B., 1978. Time and space scanning of the b-value a method for monitoring the development of catastrophic earthquakes. Acta Geophys. Sin. 21, 101–125.
Li, X., 2001. Vertical resolution: gravity versus vertical gravity gradient. Lead. Edge 20, 901–904.
Lindquist, K., Engle, K., Stahlke, D., Price, E., 2004. Global topography and bathymetry grid improves research efforts. EOS 85 (19). http://dx.doi.org/10.1029/2004EO190003.
Llenos, A.L., Mc Guire, J.J., 2007. Influence of fore-arc structure on the extent of great subduction zone earthquakes. J. Geophys. Res. 112, B09301.
Lomnitz, C., 2004. Major earthquakes of Chile: a historical survey, 1535–1960. Seismol. Res. Lett. 75, 368–378.
Maksymowicz, A., Tréhuc, A., Contreras-Reyes, E., Ruiz, S., 2015. Density-depth model of the continental wedge at the maximum slip segment of the Maule Mw8.8 megathrust earthquake. Earth Planet. Sci. Lett. 409, 265–277. http://dx.doi.org/10.1016/j.epsl.2014.11.005.
Metois, M., Socquet, A., Vigny, C., Carrizo, D., Peyrat, S., Delorme, A., Maureira, E., Valderas-Bermejo, M.C., Ortega, I., 2013. Revisiting the North Chile seismic gap segmentation using GPS-derived interseismic coupling. Geophys. J. Int. 194, 1283–1294.
Moreno, M., Bartsch, M., Zhang, Y., Oncken, O., Tilmann, F., Dahm, T., Victor, P., Barrientos, S., Vilotte, J.P., 2014. Gradual unlocking of plate boundary controlled initiation of the 2014 Iquique earthquake. Nature 512, 299–302. http://dx.doi.org/10.1038/nature13681.
Moreno, M.S., Melnick, D., Rosenau, M., Baez, J., Klotz, J., Oncken, O., Tassara, A., Chen, J., Bataille, K., Bevis, M., Socquet, A., Bolte, J., Vigny, C., Brooks, B., Ryder, I., Grund, V., Smalley, B., Carrizo, D., Bartsch, M., Hase, H., 2012. Toward understanding tectonic control on the Mw 8.8 2010 Maule Chile earthquake. . Earth Planet. Sc. Lett. 321, 152–165. http://dx.doi.org/10.1016/j.epsl.2012.01.006.
Nishenko, S.P., 1985. Seismic potential for large and great interplate earthquakes along the Chilean and southern Peruvian margins of South America. A quantitative reappraisal. J. Geophys. Res. 90, 3589–3615.
Ohnaka, M., Mogi, K., 1982. Frequency characteristics of acoustic emission in rocks under uniaxial compression and its relation to the fracturing process to failure. J. Geophys. Res. 87 (B5), 3873–3884.
Page, M.T., Custódio, S., Archuleta, R.J., Carlson, J.M., 2009. Constraining earthquake source inversions with GPS data: 1. Resolution-based removal of artifacts. J. Geophys. Res. 114, B01314. http://dx.doi.org/10.1029/2007JB005449.
Pail, R., Bruisma, S., Migliaccio, F., Förste, C., Goiginger, H., Schuh, W.D., Höck, E., Reguzzoni, M., Brockmann, J.M., Abrikosov, O., Veicherts, M., Fecher, T., Mayrhofer, R., Krasbutter, I., Sansò, F., Tscherning, C.C., 2011. First GOCE gravity field models derived by three different approaches. J. Geod. 85, 819–843.
Panet, I., Mikhailov, V., Diament, M., Pollitz, F., King, G., de Viron, O., Holschneider, M., Biancale, R., Lemoine, J.-M., 2007. Coseismic and post-seismic signatures of the Sumatra 2004 December and 2005 March earthquakes in GRACE satellite gravity. Geophys. J. Int. 171, 177–190.
Peltzer, G., Crampé, F., Rosenb, P., 2001. The Mw 7.1, Hector Mine, California earthquake: surface rupture, surface displacement field, and fault slip solution from ERS SAR data. Earth Planet. Sci. Lett. 333, 545–555.
Peyrat, S., Madariaga, R., Buforn, E., Campos, J., Asch, G., Vilotte, J.P., 2010. Kinematic rupture process of the 2007 Tocopilla earthquake and its main aftershocks from teleseismic and strong motion data. Geophys. J. Int. 182, 1411–1430. http://dx.doi.org/10.1111/j.1365-1246X.2010.04685.x.
Pollitz, F.F., Brooks, B., Tong, X., Bevis, M.G., Foster, J.H., Bürgmann, R., Smalley, R.J., Vigny, C., Socquet, A., Ruegg, J.C., Campos, J., Barrientos, S., Parra, H., Baez Soto, J.C., Cimbaro, S., Blanco, M., 2011. Coseismic slip distribution of the February 27, 2010 Mw 8.8 Maule, Chile earthquake. Geophys. Res. Lett. 38, L09309. http://dx.doi.org/10.1029/2011GL047065.
Pritchard, M.E., Norabuena, E.O., Ji, C., Boroschek, R., Comte, D., Simons, M., Dixon, T.H., Rosen, P.A., 2007. Geodetic, teleseismic, and strong motion constraints on slip from recent southern Peru subduction zone earthquakes. J. Geophys. Res. 112, B03307. http://dx.doi.org/10.1029/2006JB004294.
Ranero, C., von Huene, R., Weinrebe, W., Reichert, C., 2006. Tectonic processes along the Chile convergent margin. In: Oncken, O., Chong, G., Franz, G., Giese, P., Götze, H.J., Ramos, V.A., Strecker, M.R., Wigger, P. (Eds.), The Andes - Active Subduction Orogeny. Frontiers in Earth Science Series. Springer-Verlag, Berlin Heidelberg New York, pp. 91–121.
Ruiz, S., Metois, M., Fuenzalida, A., Ruiz, J., Leyton, F., Grandin, R., Vigny, C., Madariaga, R., Campos, J., 2014. Intense foreshocks and a slow slip event preceded the 2014 Iquique Mw=8.1 earthquake. Science 345 (6201), 1165–1169. http://dx.doi.org/10.1126/science.1256074.
Rummel, R., Yi, W., Stummer, C., 2011. GOCE gravitational gradiometry. J. Geod. 85 (11), 777–790. http://dx.doi.org/10.1007/s00190-011-0500-0.
Sallares, V., Ranero, C.R., 2005. Structure of the North Chile erosional convergent margin off Antofagasta (23°30' S). J. Geophys. Res. 110 http://dx.doi.org/10.1029/2004JB003418.
Sammonds, P.R., Meredith, P.G., Main, I.G., 1992. Role of pore fluids in the generation of seismic precursors to shear fracture. Nature 359, 228–230.
Scholl, D.W., Christensen, M.N., von Huene, R., Marlow, M.S., 1970. Peru-Chile trench sediments and sea-floor spreading. Geol. Soc. Am. Bull. 81, 1339–1360.
Scholz, C.H., 1968. The frequency-magnitude relation of micro fracturing in rock and its relation to earthquakes. Bull. Seismol. Soc. Am. 58, 388–415.
Schorlemmer, D., Wiemer, S., Wyss, M., 2005. Variations in earthquake-size distribution across different stress regimes. Nature 437, 539–542.
Schurr, B., Asch, G., Hainzl, S., Bedford, J., Hoechner, A., Palo, M., Wang, R., Moreno, M., Bartsch, M., Zhang, Y., Oncken, O., Tilmann, F., Dahm, T., Victor, P., Barrientos, S., Vilotte, J.P., 2014. Gradual unlocking of plate boundary controlled initiation of the 2014 Iquique earthquake. Nature 512, 299–302. http://dx.doi.org/10.1038/nature13681.
Shao, G., Li, X., Liu, Q., Zhao, X., Yano, T., Ji, C., 2010. Preliminary Slip Model of the Feb 27, 2010 Mw= 8.9 Maule, Chile Earthquake. www.geol.uvsb.edu/faculty/ji/big_earthquakes/2010/02/27/chile_2_27.html.
Sladen, A., Tavera, H., Simons, M., Avouac, J.P., Konca, A.O., Perfettini, H., Audin, L., Fielding, E.J., Ortega, F., 2010. Source model of the 2007 Mw 8.0 Pisco, Peru earthquake: implications for seismogenic behavior of subduction megathrusts. J. Geophys. Res. 115 (B02405) http://dx.doi.org/10.1029/2009JB006429.
Smith, W.D., 1981. The b-value as an earthquake precursor. Nature 289, 136–139.
Smith, W.D., 1986. Evidence for precursory changes in the frequency-magnitude b-value. Geophys. J. Res. Astron. Soc. 86, 815–838.
Sobiesiak, M.M., Meyer, U., Schmidt, S., Götze, H.J., Krawczyk, C., 2007. Asperity generating upper crustal sources revealed by b-value and isostatic residual anomaly grids in the area of Antofagasta. J. Geophys. Res. 112 (B12308) http://dx.doi.org/10.1029/2006JB004796.
Song, T.R., Simons, M., 2003. Large trench-parallel gravity variations predict seismogenic behavior in subduction zones. Science 301, 630–633.
Sparkes, R., Tilmann, F., Hovius, N., Hillier, J., 2010. Subducted seafloor relief stops rupture in South American great earthquakes: implications for rupture behaviour in the 2010 Maule, Chile earthquake. Earth Planet. Sci. Lett. 298, 89–94. http://dx.doi.org/10.1016/j.epsl.2010.07.029.
Stern, C.R., 1991. Role of subduction erosion in the generation of Andean magmas. Geology 19, 78–81.
Tapley, B.D., Bettadpur, S., Ries, J.C., Thompson, P.F., Watkins, M., 2004. GRACE measurements of mass variability in the earth system science. Science 305, 503–505.
Tassara, A., 2010. Control of forearc density structure on megathrust shear strength along the Chilean subduction zone. Tectonophysics 495, 34–47. http://dx.doi.org/10.1016/j.tecto.2010.06.004.
Tassara, A., Götze, H., Schmidt, S., Hackney, R., 2006. Three-dimensional density model of the Nazca plate and the Andean continental margin. J. Geophys. Res. 111 (B09404) http://dx.doi.org/10.1029/2005JB003976.
Tscherning, C.C., 1976. Computation of the second-order derivatives of the normal potential based on the representation by a legendre series. Manuscr. Geod. 1, 71–92.
Tsukakoshi, Y., Shimazaki, K., 2008. Decreased b-value prior to the M 6.2 Northern Miyagi, Japan, earthquake of 26 July 2003. Earth Planets Space 60, 915–924.
Uieda, L., Ussami, N., Braitenberg, C.F., 2010. Computation of the gravity gradient tensor due to topographic masses using tesseroids. Eos Trans. AGU 91 (26). Meeting America Supply, Abstract G22A-04. World Wide Web Address. http://

Please cite this article in press as: Álvarez, O., et al., Gradients from GOCE reveal gravity changes before Pisagua Mw = 8.2 and Iquique Mw = 7.7 large megathrust earthquakes, Journal of South American Earth Sciences (2015), http://dx.doi.org/10.1016/j.jsames.2015.09.014

code.google.com/p/tesseroids/.

Völker, D., Wiedicke, M., Ladage, S., Gaedicke, C., Reichert, C., Rauch, K., Kramer, W., Heubeck, C., 2006. Latitudinal variation in sedimentary processes in the Peru-Chile trench off Central Chile. In: Oncken, et al. (Eds.), The Andes- Active Subduction Orogeny, Frontiers in Earth Science Series, Part II. Springer-Verlag, Berlin Heidelberg New York, pp. 193–216. http://dx.doi.org/10.1007/978-3-540-48684-8_9.

von Huene, R., Scholl, D.W., 1991. Observations at convergent margins concerning sediment subduction, subduction erosion, and the growth of continental crust. Rev. Geophys. 29, 279–316.

Wang, L., Shum, C.K., Simons, F.J., Tapley, B., Dai, C., 2012. Coseismic and postseismic deformation of the 2011 Tohoku-Oki earthquake constrained by GRACE gravimetry. Geophys. Res. Lett. 39, L07301. http://dx.doi.org/10.1029/2012GL051104.

Wells, R.E., Blakely, R.J., Sugiyama, Y., Scholl, D.W., Dinterman, P.A., 2003. Basin centered asperities in great subduction zone earthquakes: a link between slip, subsidence and subduction erosion? J. Geophys. Res. 108 (B10), 2507–2536. http://dx.doi.org/10.1029/2002JB002072.

Wessel, P., Smith, W.H.F., 1998. New, improved version of the generic mapping tools released. Eos Trans. AGU 79 (47), 579.

Whittaker, J., Goncharov, A., Williams, S., Müller, R.D., Leitchenkov, G., 2013. Global sediment thickness dataset updated for the Australian-Antarctic Southern Ocean. Geochem. Geophys. Geosys. 14, 3297–3305. http://dx.doi.org/10.1002/ggge.20181.

Wild-Pfeiffer, F., 2008. A comparison of different mass element for use in gravity gradiometry. J. Geod. 82, 637–653. http://dx.doi.org/10.1007/s00190-008-0219-8.

Wyss, M., Lee, W.H.K., 1973. In: Proc. Conf in Tectonic Problems of the San Andreas Fault System, vol. 13. Stanford University, pp. 24–42.

Wyss, M., Sammis, C.G., Nadeau, R.M., Wiemer, S., 2004. Fractal dimension and b-value on creeping and locked patches of the San Andreas Fault near Parkfield, California. Bull. Seismol. Soc. Am. 94 (2), 410–421.

Yamashita, T., Knopoff, L., 1992. Model for intermediate-term precursory clustering of earthquakes. J. Geophys. Res. 97, 19873–19879.

Please cite this article in press as: Álvarez, O., et al., Gradients from GOCE reveal gravity changes before Pisagua Mw = 8.2 and Iquique Mw = 7.7 large megathrust earthquakes, Journal of South American Earth Sciences (2015), http://dx.doi.org/10.1016/j.jsames.2015.09.014